

Finite Elements with Switch Detection for Numerical Optimal Control of Nonsmooth Dynamical Systems with Set-Valued Step Functions

Armin Nurkanović^{a,1}, Anton Pozharskiy^a, Jonathan Frey^{a,b}, Moritz Diehl^{a,b}

^a*Department of Microsystems Engineering (IMTEK), University of Freiburg, Germany*

^b*Department of Mathematics, University of Freiburg, Germany*

Abstract

This paper develops high-accuracy methods for numerically solving optimal control problems subject to nonsmooth differential equations with set-valued step functions. A notable subclass of these systems are Filippov systems. The set-valued step functions are here written as the solution map of a linear program. Using the optimality conditions of this problem we rewrite the initial nonsmooth system into a equivalent dynamic complementarity systems (DCS). We extend the Finite Elements with Switch Detection (FESD) method [32], initially developed for Filippov systems transformed via Stewart's reformulation into DCS [35], to the class of nonsmooth systems with set-valued step functions. The key ideas are to start with a standard Runge-Kutta method for the obtained DCS and to let the integration step sizes to be degrees of freedom. Next, we introduce additional conditions to enable implicit but exact switch detection and to remove possible spurious degrees of freedom if no switches occur. The theoretical properties of the method are studied. Its favorable properties are illustrated on numerical simulation and optimal control examples. All methods introduced in this paper are implemented in the open-source software package NOSNOC [29].

Keywords: numerical simulation, Filippov systems, numerical optimal control, discontinuous differential equations, differential inclusions

1. Introduction

Nonsmooth dynamical systems $\dot{x} \in F(x, \Gamma(\psi(x)))$, with the set-valued Heaviside step functions $\Gamma : \mathbb{R}^{n_x} \rightarrow \mathcal{P}(\mathbb{R}^{n_\psi})$, offer an intuitive way to model many systems with Boolean relations. Here, $\psi : \mathbb{R}^{n_x} \rightarrow \mathbb{R}^{n_c}$ are *switching functions*. The set-valued step function $\gamma : \mathbb{R} \rightarrow \mathcal{P}(\mathbb{R})$ is defined as:

$$\gamma(y) = \begin{cases} \{1\}, & y > 0, \\ [0, 1], & y = 0, \\ \{0\}, & y < 0. \end{cases} \quad (1)$$

The vector-valued version of the step function, denoted by $\Gamma : \mathbb{R}^{n_x} \rightarrow \mathcal{P}(\mathbb{R}^{n_\psi})$ is the concatenation of scalar step functions, i.e., for $y \in \mathbb{R}^{n_\psi}$ we have $\Gamma(y) = (\gamma(y_1), \dots, \gamma(y_{n_\psi})) \in \mathcal{P}(\mathbb{R}^{n_\psi})$. These functions introduce discontinuities in the right-hand side (r.h.s) of the differential equation, which complicates their computational treatment. In this paper, we develop accurate and efficient numerical methods for simulation and optimization of such systems. An important subclass of nonsmooth systems with Heaviside step functions are Filippov systems [4, 15, 17]. Moreover, some classes of systems with state jumps can be reformulated

¹Corresponding author.

²This research was supported by th DFG via Research Unit FOR 2401 and project 424107692, by the EU via ELO-X 953348, by the German Federal Ministry for Economic Affairs and Climate Action (BMWK.IIC6) via the project WOpS with the project number 03EN3054A. *Email address:* {armin.nurkanovic,jonathan.frey,moritz.diehl}@imtek.uni-freiburg.de, anton.pozharskiy@merkur.uni-freiburg.de.

into Filippov systems via the time-freezing reformulation [23, 26, 28, 31]. Therefore, this modeling approach enables us to treat a broad class of practical problems.

Smoothed single-valued versions of the step function are often used in the numerical treatment of piecewise smooth systems (PSS) [10, 19, 25]. In PSS, the state space is split into nonempty regions where each of them is equipped with a different vector field. The nonsmooth set-valued step functions are used in PSS modeling to determine in which region or on what boundaries the trajectory is. A prominent application example of step functions are gene-regulatory networks [4, 25]. Another common application of step functions is to express Filippov sets in sliding modes on surfaces of co-dimension higher than one [14, 15].

The event of $x(t)$ reaching a point of discontinuity is called a *switch*. Many mature numerical simulation methods to treat ODEs with switches exist, and the theory is well-established [3]. However, numerical methods for solving optimal control problems (OCPs) subject to nonsmooth dynamical systems are not yet at such a mature stage. The key to high-accuracy methods and efficient numerical optimal control is to detect these switches in time [32]. In the control community, a popular approach to deal with the nonsmoothness is to introduce integer variables to label all modes of the nonsmooth system [9]. This leads to mixed integer optimization problems for solving OCPs. However, they often become practically intractable when nonconvexities appear or exact junction times need to be computed.

On the one hand, the computationally usually less favorable indirect methods are not widespread since Pontryagin-like conditions are not established for many classes of nonsmooth systems [20]. On the other hand, the application of direct methods, i.e., in a first-discretize-then-optimize approach, is not as straightforward as for OCPs with smooth ODEs and can lead to spurious solutions and wrong conclusions. This was first rigorously explained in the seminal paper of Stewart and Anitescu [37]. They show that in standard direct methods, the numerical sensitivities are wrong no matter how small the integrator step size is, which can result in termination at nonoptimal points [27]. Moreover, they show that the numerical sensitivities of the smoothed approximations of a nonsmooth system are only correct if the step size shrinks faster than the smoothing parameter. This makes the smoothing approach impractical, as very small step sizes are needed even for moderate accuracy.

The limitations of direct methods were recently overcome by the method of Finite Elements with Switch Detection (FESD) [32]. This method is based on standard Runge-Kutta (RK) discretizations of the Dynamic Complementarity systems (DCS), where, the integrator step sizes are left as degrees of freedom as first proposed by Baumrucker and Biegler [8]. Additional constraints are introduced to have a well-defined system with exact switch detection. The discretization yields Mathematical Programs with Complementarity Constraints (MPCC). They are highly degenerate and nonsmooth Nonlinear Programs (NLP) [34, 7]. Still, with suitable reformulations and homotopy procedures, they can be solved efficiently using techniques from smooth optimization.

FESD was initially developed for Stewart’s reformulation of Filippov systems into DCS [35]. In this paper, we extend these ideas to nonsmooth systems with set-valued step functions, which we express as solution maps of linear programs. This enables us to cover a more general class of nonsmooth ODEs with a discontinuous r.h.s. Moreover, depending on the geometry of the regions of the PSS, the step reformulation can require significantly fewer variables than Stewart’s reformulation.

Contributions. We provide a detailed study of the transformation of Filippov systems into DCS via set-valued Heaviside step functions. We study the well-posedness of the local smooth systems obtained for a fixed active set. The Filippov convex multipliers are often expressed as the product of several step functions. We propose a lifting algorithm that introduces auxiliary variables and makes the expressions less nonlinear, which can improve the convergence of the proposed method. All developments are accompanied by simple tutorial examples. Most importantly, we present the extension of the FESD method to nonsmooth systems that are described with step functions. We also extend the convergence and well-posedness results of [32] to this case. Note that the dynamical systems studied here are more general than Filippov systems. Therefore, the FESD method developed here applies to a broader class of systems. The performance of the new method is compared to the original FESD [32], and standard RK discretizations in terms of accuracy and computational time. All methods are implemented in the open-source software package NOSNOC [1].

Table 1: Key symbols used in this paper.

Symbol	Description
x	differential state, Eq. (6)
u	control function, Eq. (6)
θ	Filippov's convex multipliers
S	sign matrix defining regions R_i , (9)
α	selection of set-valued step function, (11)
λ^p	Lagrange multiplier in step DCS, (13)
λ^n	Lagrange multiplier in step DCS, (13)
β	Lifting variable in the step DCS, Sec. 4.3
$f_i(\cdot)$	modes of the PSS system, (6)
$g(\cdot)$	Stewart's indicator function, (16)
$F(\cdot)$	matrix collecting all PSS modes, (5)
$G(\cdot)$	algebraic eq. in the step DCS as nonsmooth DAE (14)
$\psi(\cdot)$	switching functions, Sec. 2.3
$\gamma(\cdot)$	scalar set-valued step function, (1)
$\Gamma(\cdot)$	vector-valued version of the step function, Eq. (1)
$W_{\mathcal{K}, \mathcal{I}}(\cdot)$	auxiliary matrix used in the study of the step DCS (13), Sec. 3.2
$B_{\mathcal{K}, \mathcal{I}}(\cdot)$	auxiliary matrix used in the study of the step DCS (13), Sec. 3.2
R_i	regions of the PSS, Eq. (6)
\tilde{R}_i	basis sets, Def. 2
\mathcal{J}	index set of PSS modes, Eq. (6)
$F_F(\cdot)$	Filippov set
$F_S(\cdot)$	Filippov set via step functions
$\mathcal{I}(\cdot)$	active set for Filippov systems, Eq. (8)
\mathcal{T}_n	n -th time interval with fixed active set $\mathcal{T}_n = (t_{s,n}, t_{s,n+1})$
\mathcal{I}_n	the fixed active set $\mathcal{I}_n = \mathcal{I}(x(t)), t \in \mathcal{I}_n$
\mathcal{I}_n^0	active set at $t_{s,n}$, i.e. $\mathcal{I}_{n,0} = \mathcal{I}(t_{s,n})$
\mathcal{C}	index set of all switching functions $c_i(x)$
\mathcal{K}	index set of all switching functions $c_i(x)$ that are zero for a given \mathcal{I} , Sec. 3.2

Outline. In Section 2, we define the nonsmooth systems of interest, the Filippov systems as their special case, and show how to transform them into equivalent DCSs. Section 3 studies the properties of these DCSs for a fixed active set and at active-set changes. Furthermore, in Section 4, we show how to efficiently model PSS with step functions and introduce a lifting algorithm to reduce the nonlinearity in the DCS. We develop the FESD method in Section 5 for nonsmooth systems with step functions. Section 6 provides convergence and well-posedness results for the new FESD method. In Section 7, we showcase the developments on several numerical examples.

Notation. The complementarity conditions for two vectors $a, b \in \mathbb{R}^n$ read as $0 \leq a \perp b \geq 0$, where $a \perp b$ means $a^\top b = 0$. For two scalar variables a, b the so-called C-functions [16] have the property $\phi(a, b) = 0 \iff a \geq 0, b \geq 0, ab = 0$. Examples are the natural residual functions $\phi_{\text{NR}}(a, b) = \min(a, b)$ or the Fischer-Burmeister function $\phi_{\text{FB}}(a, b) = a + b - \sqrt{a^2 + b^2}$. If $a, b \in \mathbb{R}^n$, we use $\phi(\cdot)$ component-wise and define $\Phi(a, b) = (\phi(a_1, b_1), \dots, \phi(a_n, b_n))$. All vector inequalities are to be understood element-wise, $\text{diag}(x) \in \mathbb{R}^{n \times n}$ returns a diagonal matrix with $x \in \mathbb{R}^n$ containing the diagonal entries. The concatenation of two column vectors $a \in \mathbb{R}^{n_a}, b \in \mathbb{R}^{n_b}$ is denoted by $(a, b) := [a^\top, b^\top]^\top$, the concatenation of several column vectors is defined analogously. A column vector with all ones is denoted by $e = (1, 1, \dots, 1) \in \mathbb{R}^n$, their dimension is clear from the context. The closure of a set C is denoted by \bar{C} , its boundary as ∂C . Given a matrix $M \in \mathbb{R}^{n \times m}$, its i -th row is denoted by $M_{i, \bullet}$ and its j -th column is denoted by $M_{\bullet, j}$. For the left and the right limits, we use the notation $x(t_s^+) = \lim_{t \rightarrow t_s, t > t_s} x(t)$ and $x(t_s^-) = \lim_{t \rightarrow t_s, t < t_s} x(t)$, respectively.

2. Nonsmooth systems with set-valued step functions

We start by showing how to rewrite a step function as a solution map of a linear program. In Section 2.2, we introduce the general differential inclusions studied in this paper. Section 2.3 specializes to Filippov systems and derives an equivalent DCS. Finally, we review Stewart's representation in Section 2.4.

2.1. Set-valued step functions

Let the switching function $\psi(x)$ be a continuous function of x , where $x : \mathbb{R} \rightarrow \mathbb{R}^{n_x}$ is some continuous function of time t . Let us denote by $\alpha \in \mathbb{R}^{n_\psi}$ a selection $\alpha \in \Gamma(\psi(x))$. A well-known way to express the function $\Gamma(\psi(x))$ [4, 8] is the use of the solution map of the parametric linear program:

$$\Gamma(\psi(x)) = \arg \min_{\alpha \in \mathbb{R}^{n_\psi}} -\psi(x)^\top \alpha \quad (2a)$$

$$\text{s.t. } 0 \leq \alpha_i \leq 1, \quad i = 1, \dots, n_\psi. \quad (2b)$$

Note that all components of α are decoupled in this LP, i.e., every α_i can be obtained by solving a one-dimensional LP with the objective $-\psi_i(x)\alpha_i$ and the feasible set $0 \leq \alpha_i \leq 1$. Let $\lambda^n, \lambda^p \in \mathbb{R}^{n_\psi}$ be the Lagrange multipliers for the lower and upper bound on α in (2b), respectively. The KKT conditions of (2) read as

$$\psi(x) = \lambda^p - \lambda^n, \quad (3a)$$

$$0 \leq \lambda^n \perp \alpha \geq 0, \quad (3b)$$

$$0 \leq \lambda^p \perp e - \alpha \geq 0, \quad (3c)$$

Let us look at a single component α_j and the associated functions $\psi_j(x)$. From the LP (2) and its KKT conditions, one can see that for $\psi_j(x) > 0$, we have $\alpha_j = 1$. Since the upper bound is active, we have that $\lambda_j^n = 0$ and from (3a) that $\lambda_{p,j} = \psi_j(x) > 0$. Likewise, for $\psi_j(x) < 0$, we obtain $\alpha_j = 0$, $\lambda_j^p = 0$ and $\lambda_j^n = -\psi_j(x) > 0$. On the other hand, $\psi_j(x) = 0$ implies that $\alpha_j \in [0, 1]$ and $\lambda_j^p = \lambda_j^n = 0$. From this discussion, it can be seen that $\psi(x)$, λ^n and λ^p are related by the following expressions:

$$\lambda^p = \max(\psi(x), 0), \quad \lambda^n = -\min(\psi(x), 0). \quad (4)$$

That is, λ^p collects the positive parts of $\psi(x)$ and λ^n the absolute value of the negative parts of $\psi(x)$. From this relation, we can immediately conclude the following:

Lemma 1. *Let $\psi(x(t))$ be a continuous function of time, then the functions $\lambda^p(t)$ and $\lambda^n(t)$ are continuous in time.*

2.2. Aizerman–Pyatnitskii differential inclusions

The set-valued step functions allow the formulation of controlled Differential Inclusions (DIs):

$$\dot{x} \in F(x, u, \Gamma(\psi(x))), \quad (5)$$

where $\psi : \mathbb{R}^{n_x} \rightarrow \mathbb{R}^{n_\psi}$ are *switching functions*. The components of the function $\Gamma(\psi(x))$ can enter in a complicated nonlinear way, and the set on the r.h.s. can be nonconvex. These systems are sometimes called Aizerman–Pyatnitskii DIs, cf. [4] and [17, page 55, Definition c]. Time-stepping methods for such systems were developed in [4]. They do not have as rich a theory as Filippov DIs, and there are fewer results available on the existence of solutions and convergence of numerical methods [4].

The commutative diagram in Figure 1 summarizes the relationships between the nonsmooth systems studied in this paper. Filippov systems arise from the convexification of ODEs with a discontinuous r.h.s., which leads to DIs with a convex and compact r.h.s.. From the derivations below, it will become apparent that Filippov systems are a special case of (5). In this paper, we focus often on piecewise smooth systems, which are a prominent subclass of ODEs with a discontinuous r.h.s.. In particular, we regard their Filippov

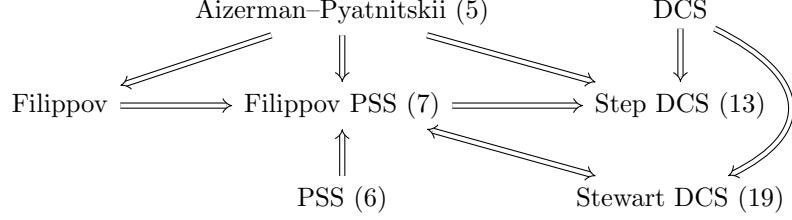


Figure 1: Summary of relations between nonsmooth systems treated in this paper.

convexification, which leads to a DI that is a special case of more general Filippov or Aizerman–Pyatnitskii systems. For computational purposes, we study DCSs that arise from the step or Stewart’s reformulation, which are in turn special cases of general DCS. Under suitable assumptions, these DCS are equivalent to Filippov PSS. The Step DCS defined below, is more general than a Filippov PSS and is under suitable assumptions equivalent to a subclass of Aizerman–Pyatnitskii systems. Such an example will be studied in Section 7.

Using the KKT system (3), the DI (5) can readily be transformed into a dynamic complementarity system. The numerical methods in this paper mainly exploit the continuity properties of the Lagrange multipliers in the KKT system and thus are directly applicable to (5). However, we restrict our theoretical studies to the case of Filippov systems, as they have a richer theory that we can build upon.

2.3. Filippov set expressed via step functions

We regard piecewise smooth systems in the form of

$$\dot{x}(t) = f_i(x(t), u(t)), \text{ if } x(t) \in R_i \subset \mathbb{R}^{n_x}, \quad i \in \mathcal{J} := \{1, \dots, n_f\}, \quad (6)$$

where R_i are disjoint, connected, and open sets. They are assumed to be nonempty and to have piecewise-smooth boundaries ∂R_i . We assume that $\bigcup_{i \in \mathcal{J}} R_i = \mathbb{R}^{n_x}$ and that $\mathbb{R}^{n_x} \setminus \bigcup_{i \in \mathcal{J}} R_i$ is a set of measure zero. The functions $f_i(\cdot)$ are assumed to be Lipschitz and at least twice continuously differentiable functions on an open neighborhood of \bar{R}_i . Furthermore, n_f is a positive integer, and $u(t)$ is a sufficiently regular externally chosen control function.

The ODE (6) is not defined on the region boundaries ∂R_i . Classical notions of solution are suitable for (6), especially if the trajectories have so-called *sliding modes*, i.e., when $x(t)$ must evolve on ∂R_i [13, 17]. Therefore, we regard Filippov’s convexification of (6). Moreover, the special structure of the PSS allows the definition of a finite number of convex multipliers θ_i , such that Filippov’s DI is defined as [17, 35]:

$$\dot{x} \in F_F(x, u) = \left\{ \sum_{i \in \mathcal{J}} f_i(x, u) \theta_i \mid \sum_{i \in \mathcal{J}} \theta_i = 1, \theta_i \geq 0, \theta_i = 0 \text{ if } x \notin \bar{R}_i, \forall i \in \mathcal{J} \right\}. \quad (7)$$

An important notion for PSS is the active set, which is defined as the set:

$$\mathcal{I}(x(t)) = \{i \in \mathcal{J} \mid \theta_i(t) > 0\}. \quad (8)$$

Note that if $x(t)$ is in the interior of a region, then \mathcal{I} is a singleton, and for sliding modes, it consists of the indices of regions neighboring the current sliding surface.

The next question to be answered is: How can we find an (implicit) function that calculates the Filippov multipliers θ for a given x ? To derive such functions, we will make use of the set-valued step functions and the definition of the regions R_i , which are expressed via the switching functions $\psi_j(x)$. We assume the functions $\psi_j(\cdot)$ to be Lipschitz continuous, sufficiently differentiable and that $\nabla \psi(x) = \frac{\partial \psi(x)}{\partial x}^\top \in \mathbb{R}^{n_x \times n_\psi}$ has rank n_ψ .

Definition 2 (Basis regions). Given n_ψ scalar switching functions $\psi_i(x)$, $i \in \mathcal{C} := \{1, \dots, n_\psi\}$, we define the 2^{n_ψ} basis regions:

$$\begin{aligned}\tilde{R}_1 &= \{x \in \mathbb{R}^{n_x} \mid \psi_1(x) > 0, \psi_2(x) > 0, \dots, \psi_{n_\psi-1}(x) > 0, \psi_{n_\psi}(x) > 0\}, \\ \tilde{R}_2 &= \{x \in \mathbb{R}^{n_x} \mid \psi_1(x) > 0, \psi_2(x) > 0, \dots, \psi_{n_\psi-1}(x) > 0, \psi_{n_\psi}(x) < 0\}, \\ &\vdots \\ \tilde{R}_{n_f} &= \{x \in \mathbb{R}^{n_x} \mid \psi_1(x) < 0, \psi_2(x) < 0, \dots, \psi_{n_\psi-1}(x) < 0, \psi_{n_\psi}(x) < 0\},\end{aligned}$$

such that $\mathbb{R}^{n_x} = \bigcup_{i=1}^{n_f} \tilde{R}_i$. These definitions are compactly expressed via a dense sign matrix $S \in \mathbb{R}^{2^{n_\psi} \times n_\psi}$:

$$S = \begin{bmatrix} 1 & 1 & \dots & 1 & 1 \\ 1 & 1 & \dots & 1 & -1 \\ \vdots & \vdots & \dots & \vdots & \vdots \\ -1 & -1 & \dots & -1 & -1 \end{bmatrix}. \quad (9)$$

The matrix S has no repeating rows and no zero entries. The sets \tilde{R}_i are defined using the rows of the matrix S :

$$\tilde{R}_i = \{x \in \mathbb{R}^{n_x} \mid S_{i,j} \psi_j(x) > 0, j \in \mathcal{C}\}, \quad i = 1, \dots, 2^{n_\psi}. \quad (10)$$

Note that the boundaries of the regions $\partial \tilde{R}_i$ are subsets of the zero-level sets of appropriate functions $\psi_j(x)$. For notation convenience and ease of exposition, we assume that the PSS regions are equal to the basis regions, i.e. $R_i = \tilde{R}_i$ for $i = 1, \dots, 2^{n_\psi}$. However, in practice, the regions of PSS may be defined as the unions of several basis sets \tilde{R}_i . In some cases, the definition of some set R_k might not depend on some of the functions $\psi_j(x)$ anymore. For example, if a region R_1 is defined as the union of the first two rows of S in (9), we obtain

$$R_1 = \tilde{R}_1 \cup \tilde{R}_2 = \{x \in \mathbb{R}^{n_x} \mid \psi_1(x) < 0, \psi_2(x) < 0, \dots, \psi_{n_\psi-1}(x) < 0\}.$$

The definition of R_1 does not depend on $\psi_{n_\psi}(x)$ anymore. Similarly, the union of $\tilde{R}_1, \tilde{R}_2, \tilde{R}_3$ and \tilde{R}_4 does not depend on $\psi_{n_\psi-1}(x)$ and $\psi_{n_\psi}(x)$. The concrete geometry of the regions R_i can reduce the number of algebraic variables in the step reformulation significantly. This is discussed in more detail in Section 4.4.

For ease of exposition, we illustrate the step representation on a simple example and give in the sequel the general expression.

Example 1 (Step representation). We regard four regions defined via two scalar switching functions $\psi_1(x)$ and $\psi_2(x)$. The regions are equal to the basis sets from Definition 2 and read as $R_1 = \{x \in \mathbb{R}^{n_x} \mid \psi_1(x) > 0, \psi_2(x) > 0\}$, $R_2 = \{x \in \mathbb{R}^{n_x} \mid \psi_1(x) > 0, \psi_2(x) < 0\}$, $R_3 = \{x \in \mathbb{R}^{n_x} \mid \psi_1(x) < 0, \psi_2(x) > 0\}$ and $R_4 = \{x \in \mathbb{R}^{n_x} \mid \psi_1(x) < 0, \psi_2(x) < 0\}$. It is not difficult to see that the matrix S read as

$$S = \begin{bmatrix} 1 & 1 \\ 1 & -1 \\ -1 & 1 \\ -1 & -1 \end{bmatrix}.$$

Furthermore, let $f_i(x)$ be the vector fields associated to the regions R_i , $i \in \{1, 2, 3, 4\}$. A selection of the Filippov set (7) and the associated ODE reads as:

$$\dot{x} = \alpha_1 \alpha_2 f_1(x) + \alpha_1 (1 - \alpha_2) f_2(x) + (1 - \alpha_1) \alpha_2 f_3(x) + (1 - \alpha_1) (1 - \alpha_2) f_4(x), \alpha \in \Gamma(\psi(x)).$$

By inspection, we determine that $\theta_1 = \alpha_1 \alpha_2$, $\theta_2 = \alpha_1 (1 - \alpha_2)$, $\theta_3 = (1 - \alpha_1) \alpha_2$, and $\theta_4 = (1 - \alpha_1) (1 - \alpha_2)$. Since $\alpha_1, \alpha_2 \in [0, 1]$ it is clear that $\theta_i \in [0, 1], i \in \{1, \dots, 4\}$. Similarly, direct calculation shows that

$\sum_{i=1}^4 \theta_i = 1$. We conclude, that we have indeed represented the Filippov set with the expression above. Observe that the entries of $S_{i,j}$ determine how α_j enters the expression for θ_i . For $S_{i,j} = 1$ we have α_j , for $S_{i,j} = -1$ we have $(1 - \alpha_j)$. This leads to multi-affine terms consisting of products of α_j and $(1 - \alpha_j)$. Next, let us verify on a few examples that θ_i also takes the correct values. For $x \in R_1$ we have that $\alpha_1 = 1$ and $\alpha_2 = 1$. In this case $\theta_1 = 1$ and $\theta_2 = \theta_3 = \theta_4 = 0$. Now let $\mathcal{I}(x) = \{1, 2\}$, that is we have a sliding mode between R_1 and R_2 , i.e., $\psi_1(x) > 0$ and $\psi_2(x) = 0$. Thus we obtain, $\theta_1 \in [0, 1]$, $\theta_2 \in [0, 1]$ and $\theta_3 = \theta_4 = 0$. The values of θ_1 and θ_2 are determined from the condition $\frac{d}{dt}\psi_2(x) = 0$.

We generalize the patterns observed in the last example and define the set

$$F_S(x) := \left\{ \sum_{i=1}^{2^{n_\psi}} \prod_{j=1}^{n_\psi} \left(\frac{1 - S_{i,j}}{2} + S_{i,j} \alpha_j \right) f_i(x) \mid \alpha \in \Gamma(\psi(x)) \right\}. \quad (11)$$

Note that we have

$$\frac{1 - S_{i,j}}{2} + S_{i,j} \alpha_j = \begin{cases} \alpha_j, & \text{if } S_{i,j} = 1, \\ 1 - \alpha_j, & \text{if } S_{i,j} = -1. \end{cases}$$

Similar definitions of $F_S(x)$ in Eq. (11) can be found in [15, Section 4.2] and [19, Section 2.1]. Next, we show that $F_S(x)$ is indeed the same set as $F_F(x)$, i.e., the set in the r.h.s. of (7).

Lemma 3 (Lemma 1.5 in [15]). *Let $a_1, a_2, \dots, a_m \in \mathbb{R}$. Consider the 2^m non-repeated products of the form $p_i = (1 \pm a_1)(1 \pm a_2) \cdots (1 \pm a_m)$, then it holds that $\sum_{i=1}^{2^m} p_i = 2^m$.*

Proposition 4. *Let*

$$\theta_i = \prod_{j=1}^{n_\psi} \left(\frac{1 - S_{i,j}}{2} + S_{i,j} \alpha_j \right), \text{ for all } i \in \mathcal{J} = \{1, \dots, n_f\}, \quad (12)$$

then it holds that $F_F(x) = F_S(x)$.

Proof. We only need to show that $\theta_i \geq 0$ for all $i \in \mathcal{J}$ and $\sum_{i \in \mathcal{J}} \theta_i = 1$. It is easy to see that $\theta_i \in [0, 1]$ as it consists of a product of terms that takes value in $[0, 1]$.

Next we show that $\sum_{i \in \mathcal{J}} \theta_i = 1$. We introduce the change of variables:

$$\frac{1 + b_j}{2} = \alpha_j, \quad \frac{1 - b_j}{2} = 1 - \alpha_j.$$

Then all θ_i are of the form

$$\theta_i = 2^{-n_\psi} \prod_{j=1}^{n_\psi} (1 \pm b_j).$$

By applying Lemma 3 we conclude that $\sum_{i \in \mathcal{J}} \theta_i = 1$ and the proof is complete. \square

To pass from the definition in Eq. (11) to a dynamic complementarity system, we state the KKT conditions of (2) to obtain an algebraic expression for $\Gamma(\psi(x))$. Combining this with the definition of the Filippov set in (11) and the expression for θ_i in (12), we obtain the following DCS:

$$\dot{x} = F(x, u) \theta, \quad (13a)$$

$$\theta_i = \prod_{j=1}^{n_\psi} \left(\frac{1 - S_{i,j}}{2} + S_{i,j} \alpha_j \right), \text{ for all } i \in \mathcal{J}, \quad (13b)$$

$$\psi(x) = \lambda^p - \lambda^n, \quad (13c)$$

$$0 \leq \lambda^n \perp \alpha \geq 0, \quad (13d)$$

$$0 \leq \lambda^p \perp e - \alpha \geq 0, \quad (13e)$$

where $F(x) = [f_1(x, u), \dots, f_{n_f}(x, u)] \in \mathbb{R}^{n_x \times n_f}$, $\theta = (\theta_1, \dots, \theta_{n_f}) \in \mathbb{R}^{n_f}$ and $\lambda^p, \lambda^n, \alpha \in \mathbb{R}^{n_\psi}$. We group all algebraic equations into a single function and use a C-function $\Psi(\cdot, \cdot)$ for the complementarity condition to obtain a more compact expression:

$$G(x, \theta, \alpha, \lambda^p, \lambda^n) := \begin{bmatrix} \theta_1 - \prod_{j=1}^{n_\psi} \left(\frac{1-S_{1,j}}{2} + S_{1,j}\alpha_j \right) \\ \vdots \\ \theta_{n_f} - \prod_{j=1}^{n_\psi} \left(\frac{1-S_{n_f,j}}{2} + S_{n_f,j}\alpha_j \right) \\ \psi(x) - \lambda^p + \lambda^n \\ \Psi(\lambda^n, \alpha) \\ \Psi(\lambda^p, e - \alpha) \end{bmatrix}. \quad (14)$$

Finally, we obtain a compact representation of (13) in the form of a nonsmooth DAE:

$$\dot{x} = F(x, u)\theta, \quad (15a)$$

$$0 = G(x, \theta, \alpha, \lambda^p, \lambda^n). \quad (15b)$$

2.4. Stewart's representation

In Stewart's representation, the regions R_i are defined via so-called indicator functions $g_i(x)$ for all $i \in \mathcal{I}$. The definition reads as [35]

$$R_i = \{x \in \mathbb{R}^{n_x} \mid g_i(x) < \min_{j \in \mathcal{J} \setminus \{i\}} g_j(x)\}. \quad (16)$$

This representation of the regions might not be the most intuitive one. However, if the regions R_i match the basis regions \tilde{R}_i from Definition 2, it was shown in [32] that the function $g(x)$ can be obtained as:

$$g(x) = -S\psi(x). \quad (17)$$

The multiplier vector θ is expressed as the solution of an LP parameterized by x :

$$\theta(x) \in \arg \min_{\tilde{\theta} \in \mathbb{R}^{n_f}} g(x)^\top \tilde{\theta} \quad (18a)$$

$$\text{s.t. } e^\top \tilde{\theta} = 1 \quad (18b)$$

$$\tilde{\theta} \geq 0. \quad (18c)$$

Using its KKT condition, one can obtain a DCS equivalent to (15), which read as:

$$\dot{x} = F(x, u)\theta, \quad (19a)$$

$$g(x) - \lambda + \mu = 0, \quad (19b)$$

$$0 \leq \lambda \perp \theta \geq 0, \quad (19c)$$

$$e^\top \theta = 1, \quad (19d)$$

where $\mu \in \mathbb{R}$ and $\lambda \in \mathbb{R}_{n_f}$ are the Lagrange multipliers for the constraints (18b) and (18c), respectively. The FESD method was initially developed for this formulation in [32].

3. Properties of the step representation DCS

In this section, we study some properties of the DCS (13) for a fixed active set and at active-set changes. These properties are useful for algorithmic development in the subsequent sections.

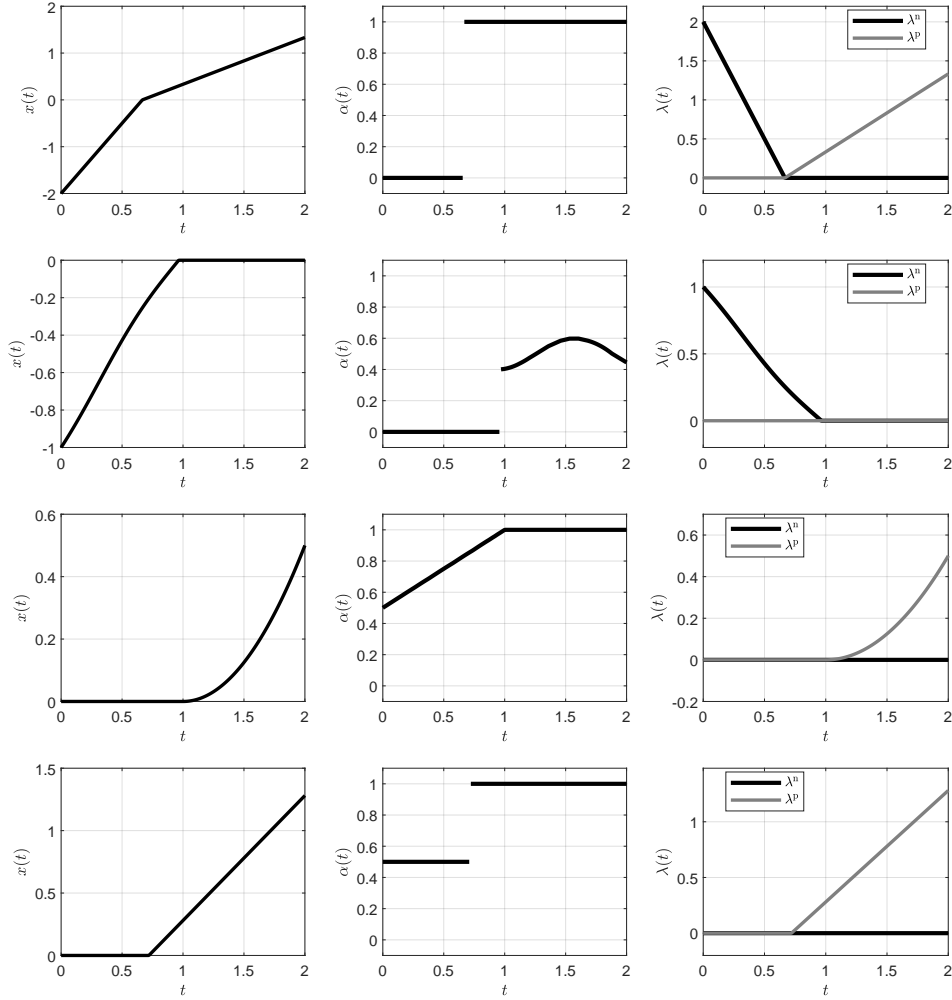


Figure 2: Illustration of example solution trajectories for different switching cases. The rows from top to bottom show $x(t)$, $\alpha(t)$, $\lambda^p(t)$ and $\lambda^n(t)$ for the cases (a)-(d) in Example 2, respectively.

3.1. Active-set changes and continuity of λ^p and λ^n

Active-set changes are paired with discontinuities in some of the algebraic variables. We have seen above that λ^p and λ^n are continuous functions of time. We can exploit this property in the development of numerical simulation methods in the next section.

At an active-set change, we have a zero-crossing of at least one of the switching functions, e.g., $\psi_j(x)$ for some j . It follows from (4) that also $\lambda_j^p(t)$ and $\lambda_j^n(t)$ must be zero at an active-set change. We use now the DCS formulation via step functions in Eq. (13) to illustrate the different switching cases that arise in Filippov systems.

Example 2. There are four possible switching cases which we illustrate with the following examples:

- (a) crossing a surface of discontinuity, $\dot{x}(t) \in 2 - \text{sign}(x(t))$,
- (b) entering a sliding mode, $\dot{x}(t) \in -\text{sign}(x(t)) + 0.2 \sin(5t)$,
- (c) leaving a sliding mode $\dot{x}(t) \in -\text{sign}(x(t)) + t$,
- (d) spontaneous switch, $\dot{x}(t) \in \text{sign}(x(t))$.

In case (a), for $x(0) < 0$ the trajectory reaches $x = 0$ and crosses it. In example (b), for any finite $x(0)$, the trajectory reaches $x = 0$ and stays there. On the other hand, in example (c), for $x(0) = 0$, the DI has a unique solution and leaves $x = 0$ at $t = 1$. In the last example, the DI has infinitely many solutions for $x(0) = 0$, and $x(t)$ can spontaneously leave $x = 0$ at any $t \geq 0$. The trajectories are illustrated in Figure 2. In all cases, the Lagrange multipliers λ^p and λ^n are zero at a switch but have nonzero left or right time derivatives.

3.2. Fixed active set in the step formulation

We study the properties of the DCS (13) for a fixed active set \mathcal{I} . Without loss of generality, the corresponding time interval is $\mathcal{T} = (0, T)$. For a fixed active set, the DCS (13) reduces either to an ODE or to a DAE.

We start with the simpler ODE case. Let $\psi_j(x) \neq 0$ for all $j \in \mathcal{C} = \{1, \dots, n_\psi\}$, then $x(t)$ is in the interior of some region R_i . It can be seen from the LP (2) that $\alpha_j \in \{0, 1\}$ for all $j \in \mathcal{C}$. This implies that $\theta_i = 1$ and $\theta_k = 0, k \neq i$. Therefore, $\mathcal{I} = \{i\}$ and in this case, the Filippov DI reduces to $\dot{x} \in F_F(x) = \{f_i(x)\}$, i.e., we have locally an ODE.

Next, we regard the case when \mathcal{I} is not a singleton. This means that we are at the boundary of two or more regions. Consequently, we have at least one $\psi_j(x) = 0$. Let us associate with \mathcal{I} the index set $\mathcal{K} = \{j \in \mathcal{C} \mid \psi_j(x) = 0\}$, i.e., the set of indices of all switching functions that are zero for a given active set \mathcal{I} .

In the sequel, we make use of the following notation. For a given vector $a \in \mathbb{R}^n$ and set $\mathcal{I} \subseteq \{1, \dots, n\}$, we define the projection matrix $P_{\mathcal{I}} \in \mathbb{R}^{|\mathcal{I}| \times n}$, which has zeros or ones as entries. It selects all component $a_i, i \in \mathcal{I}$ from the vector a , i.e., $a_{\mathcal{I}} = P_{\mathcal{I}} a \in \mathbb{R}^{|\mathcal{I}|}$ and $a_{\mathcal{I}} = [a_i \mid i \in \mathcal{I}]$.

Following the discussion from the previous section, for all nonzero $\psi_j(x)$, i.e., $j \in \mathcal{C} \setminus \mathcal{K}$, we can compute $\alpha_j \in \{0, 1\}$ via the LP (2) and $\lambda_{p,j}, \lambda_{n,j}$ via Eq. (4). Next, we have that $\lambda_{p,j} = \lambda_{n,j} = 0$ for all $j \in \mathcal{K}$. It is left to determine α_j for all $j \in \mathcal{K}$ and thus implicitly all θ_i , for all $i \in \mathcal{I}$. By fixing the already known variables in (13) we obtain the DAE:

$$\dot{x} = F_{\mathcal{I}}(x, u) \theta_{\mathcal{I}}, \quad (20a)$$

$$\theta_i - \prod_{j=1}^{n_\psi} \left(\frac{1 - S_{i,j}}{2} + S_{i,j} \alpha_j \right) = 0, \quad i \in \mathcal{I}, \quad (20b)$$

$$\psi_j(x) = 0, \quad j \in \mathcal{K}, \quad (20c)$$

where we define $F_{\mathcal{I}}(x, u) := F(x, u) P_{\mathcal{I}}^\top$, i.e., we select only the columns of $F(x, u)$ with the index $i \in \mathcal{I}$. Recall that α_j for all $j \in \mathcal{C} \setminus \mathcal{K}$ are known and thus no degrees of freedom. We keep them for ease of notation. Thus we have a DAE with $|\mathcal{I}| + |\mathcal{K}|$ unknowns, namely $\theta_{\mathcal{I}}$ and $\alpha_{\mathcal{K}}$, and $|\mathcal{I}| + |\mathcal{K}|$ algebraic equations in (20b) and (20c).

Next, we investigate conditions under which the DAE (20) is well-posed. For this purpose, we define the matrix

$$W_{\mathcal{K}, \mathcal{I}}(x) = \nabla \psi_{\mathcal{K}}(x)^\top F_{\mathcal{I}}(x) \in \mathbb{R}^{|\mathcal{K}| \times |\mathcal{I}|}$$

Moreover, we define a compact notation for the partial Jacobian $B_{\mathcal{K}, \mathcal{I}}(\alpha) \in \mathbb{R}^{|\mathcal{I}| \times |\mathcal{K}|}$ of (20b) w.r.t. to $\alpha_{\mathcal{K}}$, with the elements:

$$B_{i,j}(\alpha) := \frac{\partial}{\partial \alpha_j} \prod_{l \in \mathcal{C}} \frac{1 - S_{i,l}}{2} + S_{i,l} \alpha_l, \quad i \in \mathcal{I}, j \in \mathcal{K}.$$

Assumption 5. *Given a fixed active set $\mathcal{I}(x(t)) = \mathcal{I}$ for $t \in \mathcal{T}$, it holds that the matrix functions $W_{\mathcal{K}, \mathcal{I}}(x)$ and $B_{\mathcal{K}, \mathcal{I}}(\alpha)$ are Lipschitz continuous, and that $W_{\mathcal{K}, \mathcal{I}}(x) B_{\mathcal{K}, \mathcal{I}}(\alpha)$ has rank $|\mathcal{K}|$, i.e. it is full rank, for all $t \in \mathcal{T}$.*

Proposition 6. *Suppose that Assumption 5 holds. Given an initial value $x(0)$, the DAE (20) is of index 2 and has a unique solution for all $t \in \mathcal{T}$.*

Proof. First, we differentiate (20c) w.r.t. to t that we show to be a DAE of index 1:

$$\dot{x} = F_{\mathcal{I}}(x, u) \theta_{\mathcal{I}}, \quad (21a)$$

$$\theta_i - \prod_{j \in \mathcal{C}} \frac{1 - S_{i,j}}{2} + S_{i,j} \alpha_j = 0, \quad i \in \mathcal{I}, \quad (21b)$$

$$W_{\mathcal{K}, \mathcal{I}}(x) \theta_{\mathcal{I}} = 0. \quad (21c)$$

Next, we prove that the Jacobian of (21b)-(21c) w.r.t. to $(\theta_{\mathcal{I}}, \alpha_{\mathcal{K}})$ has rank $|\mathcal{I}| + |\mathcal{K}|$, i.e. it is an invertible matrix. We omit the dependencies on α and x for brevity. The Jacobian of (21b)-(21c) w.r.t. to $(\theta_{\mathcal{I}}, \alpha_{\mathcal{K}})$ has the form

$$A = \begin{bmatrix} I_{|\mathcal{I}|} & -B_{\mathcal{K}, \mathcal{I}} \\ W_{\mathcal{K}, \mathcal{I}} & \mathbf{0} \end{bmatrix}.$$

Suppose that there is a nonzero solution $(v, w) \in \mathbb{R}^{|\mathcal{I}|} \times \mathbb{R}^{|\mathcal{K}|}$ to

$$\begin{bmatrix} I_{|\mathcal{I}|} & -B_{\mathcal{K}, \mathcal{I}} \\ W_{\mathcal{K}, \mathcal{I}} & \mathbf{0} \end{bmatrix} \begin{bmatrix} v \\ w \end{bmatrix} = 0. \quad (22)$$

From the first line we have $v = B_{\mathcal{K}, \mathcal{I}} w$ and inserting this into the second line we have $W_{\mathcal{K}, \mathcal{I}} B_{\mathcal{K}, \mathcal{I}} w = 0$. Since the matrix $W_{\mathcal{K}, \mathcal{I}} B_{\mathcal{K}, \mathcal{I}} \in \mathbb{R}^{|\mathcal{K}| \times |\mathcal{K}|}$ has rank $|\mathcal{K}|$, the only solution to (22) is $w = 0$, and $v = Bw = 0$. Hence, A has full rank.

Now we can apply the implicit function theorem and express the algebraic variables $(\theta_{\mathcal{I}}(x), \alpha_{\mathcal{K}}(x))$ as Lipschitz functions of x . Since all involved functions are Lipschitz continuous, it follows that $\theta_{\mathcal{I}}(x)$ is Lipschitz continuous for a fixed \mathcal{I} on $t \in \mathcal{T}$. Consequently, the DAE (21) reduces to an ODE with a Lipschitz continuous r.h.s.. This enables us to apply the Picard-Lindelof Theorem to obtain the assertion of the proposition. \square

In [15], the authors make some assumptions on the signs of the entries of $W_{\mathcal{K}, \mathcal{I}}(x)$ and prove the existence, but not uniqueness, of solutions with a fixed-point argument. For the case of $|\mathcal{K}| \leq 2$, i.e., sliding modes with co-dimension one or two, and with additional assumptions on the signs of the entries of $W_{\mathcal{K}, \mathcal{I}}(x)$ they even prove the uniqueness of solutions.

Observe that for a given $x(t)$, there might be several \mathcal{I} that yield meaningful DAEs of the form of Eq. (20). This may happen when the Filippov DI does not have unique solutions, such as in Example 2 case (d).

4. Efficient modeling with step functions and variable lifting

In this section, we show how to efficiently represent common geometries of the PSS regions with the use of step functions. This is useful for reducing the complexity of the modeling process. Moreover, we introduce a lifting algorithm, which makes the multi-affine terms for the Filippov multipliers with the help of auxiliary variables less nonlinear.

4.1. Overview of expressions for θ via step functions

Table 2 provides an overview of how are the elementary algebraic expressions for the multipliers θ_i are related to the geometric definition of a region R_i . For this purpose, we regard the following two sets: $A = \{x \mid \psi_A(x) > 0\}$, $B = \{x \mid \psi_B(x) > 0\}$, and let $\alpha_A \in \gamma(\psi_A(x))$ and $\alpha_B \in \gamma(\psi_B(x))$. All other more complicated expressions can be obtained by using the one listed in Table 2.

Remark 7 (Sum of Filippov systems). *In practice, one often encounters DIs that arise from the sum of several Filippov systems. This occurs, for example, if we have multiple surfaces with friction, or multiple objects touching the same frictional surface [36]. All developments from this paper can be extended to this case and are implemented in NOSNOC. For the sake of brevity, we omit the corresponding equations and refer the reader to [32].*

Table 2: Expressions of θ_i for different definitions of R_i .

Definition of R_i	Expression for θ_i	Sketch
$R_i = A$	$\theta_i = \alpha_A$	
$R_i = A \cup B$	$\theta_i = \alpha_A + \alpha_B$	
$R_i = A \cap B$	$\theta_i = \alpha_A \alpha_B$	
$R_i = \text{int}(\mathbb{R}^{n_x} \setminus A) = \{x \mid \psi_A(x) < 0\}$	$\theta_i = 1 - \alpha_A$	
$R_i = A \setminus B$	$\theta_i = \alpha_A - \alpha_B$	

4.2. Representing unions of sets

The regions R_i may be given as unions of basis sets \tilde{R}_j . Consequently, the number of multipliers $\theta \in \mathbb{R}^{n_f}$ decreases and it holds that $n_f < 2^{n_\psi}$. For example, in the extreme case, we may have $R_1 = \tilde{R}_i$ and $R_2 = \cup_{j=1, j \neq i}^{2^{n_\psi}} \tilde{R}_j$, for some i , which significantly reduces the number of variables, with $n_f = 2$. We illustrate such a case with by a simple example and discuss the general case in the sequel.

Example 3 (Union of sets). We regard an example with two scalar switching functions $\psi_1(x)$ and $\psi_2(x)$, with the basis regions $\tilde{R}_1 = \{x \in \mathbb{R}^{n_x} \mid \psi_1(x) > 0, \psi_2(x) > 0\}$, $\tilde{R}_2 = \{x \in \mathbb{R}^{n_x} \mid \psi_1(x) > 0, \psi_2(x) < 0\}$, $\tilde{R}_3 = \{x \in \mathbb{R}^{n_x} \mid \psi_1(x) < 0, \psi_2(x) > 0\}$ and $\tilde{R}_4 = \{x \in \mathbb{R}^{n_x} \mid \psi_1(x) < 0, \psi_2(x) < 0\}$. The PSS is defined by the two regions:

$$R_1 = \cup_{i=1}^3 \tilde{R}_i = \{x \in \mathbb{R}^{n_x} \mid \psi_1(x) > 0\} \cup \{x \in \mathbb{R}^{n_x} \mid \psi_1(x) \leq 0, \psi_2(x) > 0\},$$

$$R_2 = \tilde{R}_4 = \{x \in \mathbb{R}^{n_x} \mid \psi_1(x) < 0, \psi_2(x) < 0\}.$$

It can be seen that the related Filippov system reads as $\dot{x} = \theta_1 f_1(x) + \theta_2 f_2(x)$, where

$$\theta_1 = \alpha_1 \alpha_2 + \alpha_1 (1 - \alpha_2) + (1 - \alpha_1) \alpha_2 = \alpha_1 + (1 - \alpha_1) \alpha_2,$$

$$\theta_2 = (1 - \alpha_1) (1 - \alpha_2).$$

By direct calculation, we verify that $\theta_1, \theta_2 \geq 0$ and $\theta_1 + \theta_2 = 1$. In contrast to the previous examples, the union of sets introduces a sum in the expressions for θ_1 .

We generalize the reasoning above as follows. Given n_f total regions and the matrix $F(x, u) \in \mathbb{R}^{n_x} \times \mathbb{R}^{n_F}$, where $n_F = 2^{n_\psi}$ is the number of possibly repeating columns. We define the index sets $\mathcal{F}_k = \{i \mid F_{\bullet,i}(x, u) = f_k(x, u)\}$, i.e., sets of column indices that are equal to $f_k(x, u)$. Note that if we have no unions, then $n_F = n_f$ and $\mathcal{F}_k = \{k\}$ for all $k \in \mathcal{F}$. Using these definitions, the expression for θ_i via step functions reads as:

$$\theta_i = \sum_{k \in \mathcal{F}_i} \prod_{j \in \mathcal{C}} \frac{1 - S_{k,j}}{2} + S_{k,j} \alpha_j. \quad (23)$$

4.3. A lifting algorithm for the multi-affine terms

Depending on the size of the matrix $S_{i,\bullet}$ has, the expression for θ_i in Eq. (12) might be very nonlinear since it is a product of n_ψ affine terms. To reduce the nonlinearity, we introduce auxiliary lifting variables as in the *lifted* Newton's method [5], which iterates on a larger but less nonlinear problem. We apply this approach to the expressions in Eq. (12) involving multi-affine terms with α_j . Whenever we have more than two terms in the multi-affine expression for θ_i , we introduce lifting variables β_k to end up with an equivalent formulation, which has only bilinear terms. We exploit the structure of the matrix S and derive an easy-to-implement algorithm that automates the lifting procedure. To give an idea of the final results we aim to obtain, we illustrate the lifting procedure with a simple example.

Example 4. Regard a PSS with $n_\psi = 3$ switching functions and $n_f = 8$ modes, i.e., the PSS regions match the basis sets, $R_i = \tilde{R}_i$, $i = \{1, \dots, 8\}$. The matrix $S \in \mathbb{R}^{8 \times 3}$, and the expression for the multipliers $\theta \in \mathbb{R}^8$ read as

$$S = \begin{bmatrix} 1 & 1 & 1 \\ 1 & 1 & -1 \\ 1 & -1 & 1 \\ 1 & -1 & -1 \\ -1 & 1 & 1 \\ -1 & 1 & -1 \\ -1 & -1 & 1 \\ -1 & -1 & -1 \end{bmatrix}, \quad G_F(\theta, \alpha) = \begin{bmatrix} \theta_1 - \alpha_1 \alpha_2 \alpha_3 \\ \theta_2 - \alpha_1 \alpha_2 (1 - \alpha_3) \\ \theta_3 - \alpha_1 (1 - \alpha_2) \alpha_3 \\ \theta_4 - \alpha_1 (1 - \alpha_2) (1 - \alpha_3) \\ \theta_5 - (1 - \alpha_1) \alpha_2 \alpha_3 \\ \theta_6 - (1 - \alpha_1) \alpha_2 (1 - \alpha_3) \\ \theta_7 - (1 - \alpha_1) (1 - \alpha_2) \alpha_3 \\ \theta_8 - (1 - \alpha_1) (1 - \alpha_2) (1 - \alpha_3) \end{bmatrix} = 0$$

We can introduce the lifting variable $\beta \in \mathbb{R}^4$ and obtain

$$G_\beta(\alpha, \beta) = \begin{bmatrix} \beta_1 - \alpha_1 \alpha_2 \\ \beta_2 - \alpha_1 (1 - \alpha_2) \\ \beta_3 - (1 - \alpha_1) \alpha_2 \\ \beta_4 - (1 - \alpha_1) (1 - \alpha_2) \end{bmatrix} = 0, \quad G_\theta(\theta, \alpha, \beta) = \begin{bmatrix} \theta_1 - \beta_1 \alpha_3 \\ \theta_2 - \beta_1 (1 - \alpha_3) \\ \theta_3 - \beta_2 \alpha_3 \\ \theta_4 - \beta_2 (1 - \alpha_3) \\ \theta_5 - \beta_3 \alpha_3 \\ \theta_6 - \beta_3 (1 - \alpha_3) \\ \theta_7 - \beta_4 \alpha_3 \\ \theta_8 - \beta_4 (1 - \alpha_3) \end{bmatrix} = 0$$

The equation $G_\beta(\alpha, \beta) = 0$ relates the lifting variables β_i with the α_j , whereas $G_\theta(\theta, \alpha, \beta)$ provides new expressions for θ_i via β_i and the remaining α_j . By replacing $G_F(\theta, \alpha) = 0$ with $G_{\text{lift}}(\theta, \alpha, \beta) := (G_\beta(\alpha, \beta), G_\theta(\theta, \alpha, \beta)) = 0$, we obtain an equivalent system of equations that only consists of bilinear terms.

We proceed by outlining a general lifting algorithm. The expressions for θ_i consist of the product of n_ψ affine terms. Our goal is to have at most n_d terms in the multi-affine expression for θ_i . For example, if we pick $n_d = 2$, we have only bilinear expressions in the equations defining θ and β . Thus, the parameter $n_\psi \geq n_d \geq 2$, controls the number of terms in the multi-affine expressions and implicitly the number of new lifting variables $\beta \in \mathbb{R}^{n_\beta}$. Given the matrix S , our goal is to automatically obtain the constraint $G_{\text{lift}}(\theta, \alpha, \beta) = 0$.

The algorithm outlined above can be implemented using a symbolic framework such as **CasADi** [6]. We provide the pseudo code in Algorithm 1, which introduces the lifting algebraic variables β and new *lifted*

Algorithm 1 Lifting algorithm for the step DCS (13)

```

1: Input:  $S, n_d$ 
2: Initialize:  $\tilde{S} \leftarrow S, k \leftarrow 0; \tilde{\theta} \leftarrow e \in \mathbb{R}^{n_f}, G_\theta(\theta, \alpha, \beta) \leftarrow [], G_\beta(\alpha, \beta) \leftarrow []$ .
3: for  $j = 1 : n_\psi$  do
4:    $\tilde{N} \leftarrow \sum_{j=1}^{n_\psi} |\tilde{S}_{\bullet,j}|$ 
5:    $\mathcal{I}_j \leftarrow \{i \mid \tilde{N}_i = j\}$ 
6:    $\tilde{\theta} \leftarrow \tilde{\theta} \cdot \left( \frac{e - \tilde{S}_{\bullet,j}}{2} + S_{\bullet,j}^{\text{temp}} \cdot \alpha_j \right)$ 
7:   if  $\mathcal{I}_j \neq \emptyset$  then
8:      $G_\theta(\theta, \alpha, \beta) \leftarrow (G_\theta(\theta, \alpha, \beta), \theta_{k+\mathcal{I}_j} - \tilde{\theta}_{\mathcal{I}_j})$ 
9:     Remove entries of  $\tilde{\theta}$  with index in  $\mathcal{I}_j$ 
10:    Remove rows of  $\tilde{S}$  with index in  $\mathcal{I}_j$ 
11:     $k \leftarrow k + \max(\mathcal{I}_j)$ 
12:   end if
13:   if  $j \in \{n_d, \dots, n_\psi - 1\}$  then
14:      $\{\mathcal{I}_{\text{red}}, \mathcal{I}_{\text{full}}\} = \text{unique}(\tilde{S}_{\bullet, \{1, \dots, j\}})$ ,
15:      $\beta \leftarrow (\beta, \beta^j)$  where  $\beta^j \in \mathbb{R}^{|\mathcal{I}_{\text{red}}|}$ ,
16:      $G_\beta(\alpha, \beta) \leftarrow (G_\beta(\alpha, \beta) \beta^j - \tilde{\theta}_{\mathcal{I}_{\text{red}}})$ 
17:      $\tilde{\theta} \leftarrow \beta_{\mathcal{I}_{\text{full}}}^j$ 
18:   end if
19: end for
20:  $G_{\text{Lift}}(\theta, \alpha, \beta) := (G_\theta(\theta, \alpha, \beta), G_\beta(\alpha, \beta))$ 
21: Output:  $G_{\text{Lift}}(\theta, \alpha, \beta), \beta$ 

```

expressions for θ_i , namely $G_{\text{Lift}}(\theta, \alpha, \beta)$. Note that we make use of three helper variables, the matrix \tilde{S} and the vectors $\tilde{\theta}$ and \tilde{N} . The matrix \tilde{S} is a submatrix of S , where we have removed the rows with index i , for which we already have a (lifted) expression for θ_i . The vector \tilde{N} , defined in line 4, collects the number of nonzero entries of every row \tilde{S} . In other words, it keeps track of how many terms are in the initial expressions for θ_i , that are not yet lifted.

The main loop iterates from $j = 1$ to n_ψ and provides in every iteration the expressions for all θ_i that have exactly j terms in their multi-affine expression. The index set $\mathcal{I}_j = \{i \mid \tilde{N}_i = j\}$, defined in line 5, contains the indices of θ , that have exactly j entries in their corresponding multi-affine expression. In line 6, we define the auxiliary variable $\tilde{\theta}$, which stores the intermediate expressions for θ with up to j terms in the product. The index k stores the index of the last θ_k for which a lifted expression was derived. For $j \leq n_d$ the expressions for θ_i are unaltered. This is treated in lines 7-11.

As soon as $j > n_d$, the algorithm introduces new lifting variables β^j (line 15) and changes the expression for $\tilde{\theta}$ accordingly. This is done in lines 13-17. A key tool is the function **unique** in line 14. It is available in **MATLAB** and in the **numpy** package in **python**. It works as follows, given a matrix $A \in \mathbb{R}^{m \times n}$ it returns the matrix $\tilde{A} \in \mathbb{R}^{p \times n}$, with $p \leq m$. This is the matrix constructed from A by removing its repeating rows. More importantly for our needs, it returns the index sets \mathcal{I}_{red} and $\mathcal{I}_{\text{full}}$, with $|\mathcal{I}_{\text{red}}| = p$ and $|\mathcal{I}_{\text{full}}| = m$. The index sets have the properties $A = [\tilde{A}_{i,\bullet} \mid i \in \mathcal{I}_{\text{full}}] \in \mathbb{R}^{m \times n}$ and $\tilde{A} = [\tilde{A}_{i,\bullet} \mid i \in \mathcal{I}_{\text{red}}] \in \mathbb{R}^{p \times n}$.

This enables the use of the same β^j for several θ_i if they share the same terms in the corresponding multi-affine expressions, cf. lines 15-17. After the loop is finished, the algorithm outputs $G_{\text{Lift}}(\theta, \alpha, \beta)$ and β . One can verify that Algorithm 1 produces the same output as Example 4. It can be shown, that for a given $n_d < n_\psi$, the total number of new lifting variables is $n_\beta = 2^{n_\psi} - 2^{n_d}$.

4.4. Comparisons of Stewart's and the step reformulation

We compare Stewart's reformulation (19) and the step reformulation (13) based on their total number of algebraic variables, complementarity constraints, and equality constraints for a given number of switching

Table 3: Comparisons of the problem sizes in Stewart's and the step reformulation for a fixed n_ψ .

Ref.	n_f	n_β	n_{alg}	n_{comp}	n_{eq}
Stewart	2^{n_ψ}	0	$2 \cdot 2^{n_\psi} + 1$	2^{n_ψ}	$2^{n_\psi} + 1$
Step	$[2, 2^{n_\psi}]$	$\begin{cases} 2^{n_\psi} - 2^{n_d}, & n_d \leq n_\psi \\ 0, & n_d > n_\psi \end{cases}$	$n_f + 3n_\psi + n_\beta$	$2n_\psi$	$n_\psi + n_\beta + n_f$

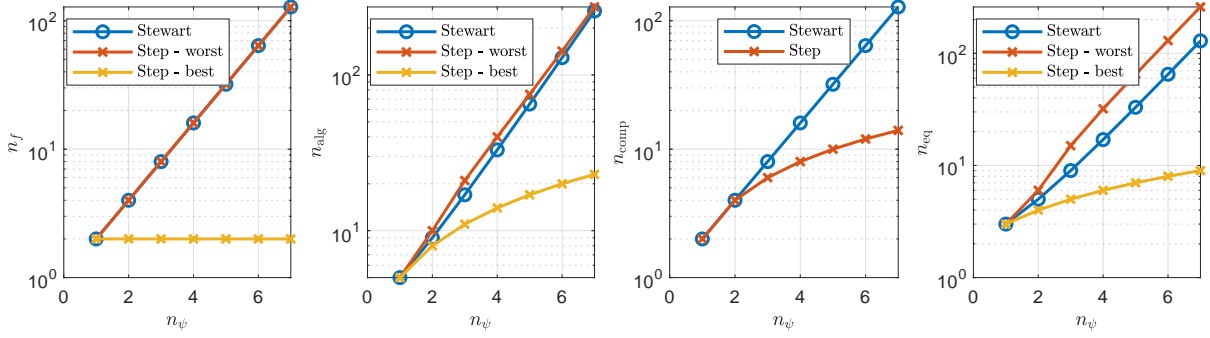


Figure 3: Comparisons of the complexities of Stewart's and the step reformulation.

functions n_ψ . The total number of regions (and multipliers θ_i) in Stewart's reformulation is always $n_f = 2^{n_\psi}$. In this reformulation, in order to reduce the number of multipliers θ_i , we cannot exploit the setting if regions R_i are defined as unions of basis sets \tilde{R}_j , cf. Section 2.4. On the other hand, in the step reformulation, depending on the geometry of the regions R_i , n_f is an integer in $[2, 2^{n_\psi}]$. In the step reformulation, we may introduce n_β lifting variables to reduce the nonlinearity. If $n_d > n_\psi$, this leads to $n_\beta = 2^{n_\psi} - 2^{n_d}$ additional lifting variables and equations.

Regarding the number of algebraic variables, in Stewart's reformulation, we have $\lambda \in \mathbb{R}^{2^{n_\psi}}$ and $\mu \in \mathbb{R}$. In the step reformulation, we have $\alpha, \lambda^p, \lambda^n \in \mathbb{R}^{n_\psi}$. Thus, the total number of algebraic variables in the former case is $n_{\text{alg}} = 2 \cdot 2^{n_\psi} + 1$, and in the later case $n_{\text{alg}} = n_f + 3n_\psi + n_\beta$. The number of complementarity constraints n_{comp} in Stewart's case is $n_{\text{comp}} = 2^{n_\psi}$, and in the step case $n_{\text{comp}} = 2n_\psi$, i.e., we have exponential versus linear complexity. Finally, in Stewart's reformulation, we have in total $n_{\text{eq}} = 2^{n_\psi} + 1$ equality constraints ($g_i(x) = \lambda_i - \mu$ and $e^\top \theta = 1$). In the step case, we have $n_{\text{eq}} = n_f + n_\beta + n_\psi$ constraints, for the definitions of θ_i , β_i and the constraints $\psi_i(x) = \lambda_i^p - \lambda_i^n$, respectively. The numbers of variables and constraints are summarized in Table 3.

Figure 3 illustrates the different quantities for several n_ψ . We plot for the step reformulation two extreme scenarios:

1. Worst complexity case - every basis set defines a PSS region, $n_f = 2^{n_\psi}$, we lift to have only bilinear terms, i.e., $n_d = 2$ (maximizes the number of lifting variables).
2. Best complexity case - o no lifting and only two regions ($n_f = 2$) for all n_ψ .

Note that in both cases the step reformulation has the same number of complementarity constraints. For smaller values of n_ψ , both reformulations have similar complexity. For a large number of switching functions, the step reformulation has fewer variables. However, if there is no lifting, the problem might become very nonlinear for large n_ψ .

5. Finite Elements with Switch Detection (FESD) for the step representation

We start the description of FESD with the RK discretization for the step reformulation DCS. We introduce the cross complementarity and integration step size equilibration conditions for this formulation. The section finishes by showing how to discretize OCPs with the novel FESD method.

5.1. Standard implicit Runge-Kutta discretization

As a starting point in our analysis, we regard a standard RK discretization of the DCS (13). For ease of notation, we work with the nonsmooth DAE formulation of the DCS (15), which restate for convenience

$$\dot{x} = F(x, u)\theta, \quad (24a)$$

$$0 = G(x, \theta, \alpha, \lambda^p, \lambda^n) \quad (24b)$$

In the sequel, one should keep in mind that (24b) collects all algebraic equations including the complementarity conditions (13d)-(13e).

We regard a single control interval $[0, T]$ with a constant externally chosen control input $q \in \mathbb{R}^{n_u}$, i.e., we set $u(t) = q$ for $t \in [0, T]$. In Section 5.5, we will treat the discretization of OCPs with multiple control intervals. Let $x(0) = s_0$ be the initial value. The control interval $[0, T]$ is divided into N_{FE} finite elements $[t_n, t_{n+1}]$ via the grid points $0 = t_0 < t_1 < \dots < t_{N_{\text{FE}}} = T$. On each of the finite elements we regard an n_s -stage Runge-Kutta method which is characterized by the Butcher tableau entries $a_{i,j}$, b_i and c_i with $i, j \in \{1, \dots, n_s\}$ [22]. The step-sizes read as $h_n = t_{n+1} - t_n$, $n = 0, \dots, N_{\text{FE}} - 1$. The approximation of the differential state at the grid points t_n is denoted by $x_n \approx x(t_n)$.

We regard the differential representation of the Runge-Kutta method. Thus, the derivatives of states at the stage points $t_{n,i} := t_n + c_i h_n$, $i = 1, \dots, n_s$, are degrees of freedom. For a single finite element, we summarize them in the vector $V_n := (v_{n,1}, \dots, v_{n,n_s}) \in \mathbb{R}^{n_s n_x}$. The stage values for the algebraic variables are collected in the vectors: $\Theta_n := (\theta_{n,1}, \dots, \theta_{n,n_s}) \in \mathbb{R}^{n_s n_f}$, $A_n := (\alpha_{n,1}, \dots, \alpha_{n,n_s}) \in \mathbb{R}^{n_s n_c}$, $\Lambda_n^p := (\lambda_{n,1}^p, \dots, \lambda_{n,n_s}^p) \in \mathbb{R}^{n_s n_c}$ and $\Lambda_n^n := (\lambda_{n,1}^n, \dots, \lambda_{n,n_s}^n) \in \mathbb{R}^{n_s n_c}$.

We collect all *internal* variables in the vector $Z_n = (x_n, \Theta_n, A_n, \Lambda_n^p, \Lambda_n^n, V_n)$. The vector x_n^{next} denotes the state value at t_{n+1} , which is obtained after a single integration step. Now, we can state the RK equations for the DCS (24) for a single finite element as

$$0 = G_{\text{rk}}(x_n^{\text{next}}, Z_n, h_n, q) := \begin{bmatrix} v_{n,1} - F(x_n + h_n \sum_{j=1}^{n_s} a_{1,j} v_{n,j}, q) \theta_{n,1} \\ \vdots \\ v_{n,n_s} - F(x_n + h_n \sum_{j=1}^{n_s} a_{n_s,j} v_{n,j}, q) \theta_{n,n_s} \\ G(x_n + h_n \sum_{j=1}^{n_s} a_{1,j} v_{n,j}, \theta_{n,1}, \alpha_{n,1}, \lambda_{n,1}^p, \lambda_{n,1}^n) \\ \vdots \\ G(x_n + h_n \sum_{j=1}^{n_s} a_{n_s,j} v_{n,j}, \theta_{n,n_s}, \alpha_{n,n_s}, \lambda_{n,n_s}^p, \lambda_{n,n_s}^n) \\ x_n^{\text{next}} - x_n - h_n \sum_{i=1}^{n_s} b_i v_{n,i} \end{bmatrix}. \quad (25)$$

Next, we summarize the equations for all N_{FE} finite elements over the entire interval $[0, T]$ in a discrete-time system format. To make it more manageable, we use some additional shorthand notation and group all variables of all finite elements for a single control interval into the following vectors: $\mathbf{x} = (x_0, \dots, x_{N_{\text{FE}}}) \in \mathbb{R}^{(N_{\text{FE}}+1)n_x}$, $\mathbf{V} = (V_0, \dots, V_{N_{\text{FE}}-1}) \in \mathbb{R}^{N_{\text{FE}} n_s n_x}$ and $\mathbf{h} := (h_0, \dots, h_{N_{\text{FE}}-1}) \in \mathbb{R}^{N_{\text{FE}}}$. Recall that the simple continuity condition $x_{n+1} = x_n^{\text{next}}$ holds. We collect the stage values of the Filippov multipliers in the vector $\Theta = (\Theta_0, \dots, \Theta_{N_{\text{FE}}-1}) \in \mathbb{R}^{n_\theta}$ and $n_\theta = N_{\text{FE}} n_s n_f$. Similarly, we group the stage values of the algebraic variables specific to the step representation in vectors $\mathbf{A}, \mathbf{\Lambda}^p, \mathbf{\Lambda}^n \in \mathbb{R}^{n_\alpha}$, where $n_\alpha = N_{\text{FE}} n_s n_c$. Finally, we collect all internal variables in the vector $\mathbf{Z} = (\mathbf{x}, \mathbf{V}, \Theta, \mathbf{A}, \mathbf{\Lambda}^p, \mathbf{\Lambda}^n) \in \mathbb{R}^{n_z}$, where $n_z = (N_{\text{FE}} + 1)n_x + N_{\text{FE}} n_s n_x + n_\theta + 3n_\alpha$.

All computations over a single control interval of the standard discretization (denoted by the subscript *std* in the corresponding functions) are summarized in the following equations:

$$s_1 = F_{\text{std}}(\mathbf{Z}), \quad (26a)$$

$$0 = G_{\text{std}}(\mathbf{Z}, \mathbf{h}, s_0, q), \quad (26b)$$

where $s_1 \in \mathbb{R}^{n_x}$ is the approximation of $x(T)$ and

$$F_{\text{std}}(\mathbf{Z}) = x_{N_{\text{FE}}},$$

$$G_{\text{std}}(\mathbf{Z}, \mathbf{h}, s_0, q) := \begin{bmatrix} x_0 - s_0 \\ G_{\text{rk}}(x_1, Z_0, h_0, q) \\ \vdots \\ G_{\text{rk}}(x_{N_{\text{FE}}}, Z_{N_{\text{FE}}-1}, h_{N_{\text{FE}}-1}, q) \end{bmatrix}.$$

In (26), \mathbf{h} is a given parameter and implicitly fixes the discretization grid. In contrast to standard RK discretizations, we will now proceed by letting \mathbf{h} be degrees of freedom and introduce the cross-complementarity conditions for the step reformulation.

5.2. Cross complementarity

For ease of exposition, suppose that the underlying RK scheme satisfies $c_{n_s} = 1$, e.g., this holds for Radau and Lobatto schemes [22]. This means that the right boundary point of a finite element is a stage point, since $t_{n+1} = t_n + c_{n_s} h_n$. We provide extensions for $c_{n_s} \neq 1$, at the end of the section.

The goal is to derive additional constraints that will allow active-set changes only at the boundary of a finite element. Moreover, in this case, the step-size h_n should adapt such that the switch is detected exactly. Recall that for the step reformulation at every stage point we have the complementarity conditions:

$$0 \leq \lambda_{n,m}^n \perp \alpha_{n,m} \geq 0, \quad \text{for all } n \in \{1, \dots, N_{\text{FE}}\}, m \in \{1, \dots, n_s\}, \quad (27a)$$

$$0 \leq \lambda_{n,m}^p \perp e - \alpha_{n,m} \geq 0, \quad \text{for all } n \in \{1, \dots, N_{\text{FE}}\}, m \in \{1, \dots, n_s\}. \quad (27b)$$

As a first step, we exploit the continuity of the Lagrange multipliers λ^p and λ^n , cf. Section 3.1. We regard the boundary values of the approximation of λ^p and λ^n on an interval $[t_n, t_{n+1}]$. They are denoted by $\lambda_{n,0}^p$, $\lambda_{n,0}^n$ (which we define below) at t_n and λ_{n,n_s}^p , λ_{n,n_s}^n at t_{n+1} .

Next, we impose a continuity condition for the discrete-time versions of λ^p and λ^n for all $n \in \{0, \dots, N_{\text{FE}} - 1\}$:

$$\lambda_{n+1,0}^p = \lambda_{n,n_s}^p, \quad \lambda_{n+1,0}^n = \lambda_{n,n_s}^n. \quad (28)$$

Note that $\lambda_{0,0}^p$ and $\lambda_{0,0}^n$ are not defined via Eq. (28), as we do not have a preceding finite element for $n = 0$. Nevertheless, they are crucial for determining the active set in the first finite element. They are not degrees of freedom but parameters determined by a given x_0 . Using equation (4) we obtain $\lambda_{0,0}^p = \max(\psi(x_0), 0)$ and $\lambda_{0,0}^n = -\min(\psi(x_0), 0)$.

We have seen in Section 3.1 that, due to continuity, $\lambda_i^p(t)$ and $\lambda_i^n(t)$ must be zero at an active set change. Moreover, on an interval $t \in (t_n, t_{n+1})$ with a fixed active set, the components of these multipliers are either zero or positive on the whole interval. The discrete-time counterparts, i.e., the stage values $\lambda_{n,m}^p$ and $\lambda_{n,m}^n$ should satisfy these properties as well. We achieve these goals via the cross complementarity conditions, which read for all $n \in \{0, \dots, N_{\text{FE}} - 1\}$ as:

$$0 = \text{diag}(\lambda_{n,m'}^n) \alpha_{n,m}, \quad \text{for all } m \in \{1, \dots, n_s\}, m' \in \{0, \dots, n_s\}, m \neq m'. \quad (29a)$$

$$0 = \text{diag}(\lambda_{n,m'}^p) (e - \alpha_{n,m}), \quad \text{for all } m \in \{1, \dots, n_s\}, m' \in \{0, \dots, n_s\}, m \neq m'. \quad (29b)$$

In contrast to Eq. (28), here we have conditions relating variables corresponding to different RK stages within a finite element. Eq. (29) extends the complementarity conditions for the same RK-stage, i.e., for $m = m'$, which are part of the standard RK equations, cf. Eq. (27).

Some of the claims about the constraints (29) are formalized by the next lemma. Recall that in our notation $\alpha_{n,m,j}$ is the j -th component of the vector $\alpha_{n,m}$.

Lemma 8. *Regard a fixed $n \in \{0, \dots, N_{\text{FE}} - 1\}$ and a fixed $j \in \mathcal{C}$. If any $\alpha_{n,m,j}$ with $m \in \{1, \dots, n_s\}$ is positive, then all $\lambda_{n,m',j}^n$ with $m' \in \{0, \dots, n_s\}$ must be zero. Conversely, if any $\lambda_{n,m',j}^n$ is positive, then all $\alpha_{n,m,j}$ are zero.*

Proof. Let $\alpha_{n,m,i}$ be positive, and suppose $\lambda_{n,j,i}^n = 0$ and $\lambda_{n,k,i}^n > 0$ for some $k, j \in \{0, \dots, n_s\}, k \neq j$, then $\alpha_{n,m,i} \lambda_{n,k,i}^n > 0$ which violates (29), thus all $\lambda_{n,m',i}^n = 0, m' \in \{0, \dots, n_s\}$. The converse is proven similarly. \square

An analogous statement holds for $\lambda_{n,m}^p$ and $(e - \alpha_{n,m})$.

It is now left to discuss why the boundary points $\lambda_{n+1,0}^p = \lambda_{n,0}^p$ and $\lambda_{n+1,0}^n = \lambda_{n,0}^n$ of the previous finite element are included in the cross complementarity conditions (29). It turns out, they are the key to switch detection. A consequence of Lemma 8 is that, if the active set changes in the j -th component between the n -th and $(n+1)$ -st finite element, then it must hold that $\lambda_{n,n_s,j}^p = \lambda_{n+1,0,j}^p = 0$ and $\lambda_{n,n_s,j}^n = \lambda_{n+1,0,j}^n = 0$. Since $x_n^{\text{next}} = x_{n+1}$, we have from (25) the condition

$$\psi_j(x_{n+1}) = 0,$$

which defines the switching surface between two regions. Therefore, we have implicitly a constraint that forces h_n to adapt such that the switch is detected exactly.

For clarity, the conditions (29) are given in their sparsest form. However, the nonnegativity of $\alpha_{n,m}, \lambda_{n,m}^p$ and $\lambda_{n,m}^n$ allows many equivalent and more compact forms. For instance, we can use inner products instead of component-wise products or we can even summarize all constraints for a finite element, or for all finite elements in a single equation. In the sequel, we use a formulation where, together with the constraint $\sum_{n=0}^{N_{\text{FE}}-1} h_n = T$, we have the same number of new equations as new degrees of freedom by varying h_n . Thus, we combine constraints of two neighboring finite elements and have the compact formulation

$$G_{\text{cross}}(\mathbf{A}, \mathbf{\Lambda}^p, \mathbf{\Lambda}^n) = 0 \quad (30)$$

whose entries are for all $n \in \{0, \dots, N_{\text{FE}} - 2\}$ given by

$$G_{\text{cross},n}(\mathbf{A}, \mathbf{\Lambda}^p, \mathbf{\Lambda}^n) = \sum_{k=n}^{n+1} \left(\sum_{m=1}^{n_s} \sum_{\substack{m'=0, \\ m' \neq m}}^{n_s} \alpha_{k,m}^\top \lambda_{k,m'}^n + (e - \alpha_{k,m})^\top \lambda_{k,m'}^p \right).$$

We remind the reader that we use this seemingly complicated form only to obtain a square system of equations. This simplifies the study of the well-posedness of the FESD equations later. However, in an implementation one can use any of the equivalent, more sparse, or dense formulations. Many possible variants are implemented in NOSNOC [29], and the user can control the sparsity.

5.3. Step size equilibration

To complete the derivation of the FESD method for the step reformulation (24), we need to derive the step equilibration conditions. Here, *step* is referred to the integration step size and is not to be confused with the set-valued step function.

If no active-set changes happen, the cross complementarity constraints (29) are implied by the standard complementarity conditions (27). Therefore, we end up with a system of equations with more degrees of freedom than conditions. The step equilibration constraints aim to remove the degrees of freedom in the appropriate h_n if no switches happen. This results in a piecewise uniform discretization grid for the differential and algebraic states on the considered time interval.

We achieve the goals outlined above via the equation:

$$0 = G_{\text{eq}}(\mathbf{h}, \mathbf{A}, \mathbf{\Lambda}^p, \mathbf{\Lambda}^n) := \begin{bmatrix} (h_1 - h_0)\eta_1(\mathbf{A}, \mathbf{\Lambda}^p, \mathbf{\Lambda}^n) \\ \vdots \\ (h_{N_{\text{FE}}-1} - h_{N_{\text{FE}}-2})\eta_{N_{\text{FE}}-1}(\mathbf{A}, \mathbf{\Lambda}^p, \mathbf{\Lambda}^n) \end{bmatrix}, \quad (31)$$

where η_n is an indicator function that is zero only if a switch occurs, otherwise its value is strictly positive. This provides a condition that removes the spurious degrees of freedom. In the remainder of this section, we derive a possible expression for η_n .

Table 4: Overview of switching cases for the step size equilibration

Switching case	$\sigma_n^{\lambda^n, \text{B}}$	$\sigma_n^{\lambda^n, \text{F}}$	$\sigma_n^{\lambda^p, \text{B}}$	$\sigma_n^{\lambda^p, \text{F}}$	$\pi_n^{\lambda^n}$	$\pi_b^{\lambda^p}$	v_n
No switch	1	1	0	0	1	0	1
Crossing	1	0	0	1	0	0	0
Entering sliding mode	1	0	0	0	0	0	0
Leaving sliding mode	0	0	0	1	0	0	0
Spontaneous switch	0	0	0	1	0	0	0

The derivations below are motivated by the following facts. Let t_n be a switching point with $\psi_j(x(t_n)) = 0$ for some $j \in \mathcal{C}$. Consequently, it holds that $\lambda_j^p(t_n) = \lambda_j^n(t_n) = 0$. If, for example, a switch occurs at $t_{s,n}$ such that $\psi(x(t_{s,n}^-)) < 0$ and $\psi(x(t_{s,n}^+)) > 0$, we have that $\dot{\lambda}_j^n(t_{s,n}^-) < 0$, $\dot{\lambda}_j^p(t_{s,n}^-) = 0$ and that $\dot{\lambda}_j^n(t_{s,n}^+) = 0$, $\dot{\lambda}_j^p(t_{s,n}^+) > 0$. The symmetric case is possible as well. The absolute values of these directional derivatives help us to encode the switching logic. This state of affairs can be seen in Figure 2.

Now, instead of looking at the time derivatives, in the discrete-time case, we exploit the non-negativity of $\lambda_{n,m}^p$, $\lambda_{n,m}^n$, and the fact that the active set is fixed for the whole finite element. For $n \in \{1, \dots, N_{\text{FE}} - 1\}$, we define the following backward and forward sums of the stage values over the neighboring finite elements $[t_{n-1}, t_n]$ and $[t_n, t_{n+1}]$:

$$\begin{aligned} \sigma_n^{\lambda^p, \text{B}} &= \sum_{m=0}^{n_s} \lambda_{n-1,m}^p, & \sigma_n^{\lambda^p, \text{F}} &= \sum_{m=0}^{n_s} \lambda_{n,m}^p, \\ \sigma_n^{\lambda^n, \text{B}} &= \sum_{m=0}^{n_s} \lambda_{n-1,m}^n, & \sigma_n^{\lambda^n, \text{F}} &= \sum_{m=0}^{n_s} \lambda_{n,m}^n. \end{aligned}$$

They are zero if the left and right time derivatives are zero, respectively. Likewise, they are positive when the left and right time derivatives are nonzero.

Moreover, for all $n \in \{1, \dots, N_{\text{FE}} - 1\}$ we define the following variables to summarize the logical dependencies:

$$\begin{aligned} \pi_n^{\lambda^n} &= \text{diag}(\sigma_n^{\lambda^n, \text{B}}) \sigma_n^{\lambda^n, \text{F}} \in \mathbb{R}^{n_\psi}, \\ \pi_n^{\lambda^p} &= \text{diag}(\sigma_n^{\lambda^p, \text{B}}) \sigma_n^{\lambda^p, \text{F}} \in \mathbb{R}^{n_\psi}, \end{aligned}$$

and

$$v_n = \pi_n^{\lambda} + \pi_n^{\alpha} \in \mathbb{R}^{n_\psi}.$$

The switching cases and sign logic is summarized in Table 4. For readability, we put in the table a one if a variable is positive and a zero if it is zero. Let us discuss how the variables above encode the switching logic, and for this purpose, we regard the j -th switching functions $\psi_j(x)$. If no switch occurs, and for example, we have that $\psi_j(x(t)) < 0$ during the regard time interval, it follows that $\lambda_j^n(t) > 0$ and $\lambda_j^p(t) = 0$ during this time interval. In the discrete time setting, we have $\sigma_{n,j}^{\lambda^n, \text{B}}, \sigma_{n,j}^{\lambda^n, \text{F}} > 0$ and $\sigma_{n,j}^{\lambda^p, \text{B}} = \sigma_{n,j}^{\lambda^p, \text{F}} = 0$. This means that $\pi_{n,j}^{\lambda^n} > 0$, $\pi_{n,j}^{\lambda^p} = 0$ and $v_{n,j} > 0$. It can be seen that the symmetric case with $\psi_j(x(t)) > 0$ leads also to $v_{n,j} > 0$, hence we do not enumerate all symmetric cases in Table 4.

On the other hand, if we have a switch of the crossing type (cf. top plots in Figure 2 with $\psi_j(x(t)) < 0$ for $t < t_{s,n}$ and $\psi_j(x(t)) > 0$ for $t > t_{s,n}$), it follows that $\lambda_j^n(t) < 0$, $\lambda_j^p(t) = 0$ for $t < t_{s,n}$ and $\lambda_j^n(t) = 0$, $\lambda_j^p(t) > 0$ for $t > t_{s,n}$. In the discrete-time setting we obtain the sign pattern as in the second row of Table 4, with $v_{n,j} = 0$.

In general, if there is an active-set change in the j -th complementarity pair, then at most one of the j -th components of $\sigma_n^{\lambda^p, \text{B}}$ and $\sigma_n^{\lambda^p, \text{F}}$, or $\sigma_n^{\lambda^n, \text{B}}$ and $\sigma_n^{\lambda^n, \text{F}}$ is nonzero. In these cases, we obtain that $v_{n,j} = 0$, and if now switch happens we have that $v_{n,j} > 0$.

In other words, $v_{n,j}$ is only zero if there is an active-set change in the j -th complementarity pair at t_n , otherwise, it is strictly positive. We summarize all logical relations for all switching functions into a single scalar expression and define

$$\eta_n(\mathbf{A}, \mathbf{\Lambda}^p, \mathbf{\Lambda}^n) := \prod_{i=1}^{n_\psi} (v_n)_i.$$

It is zero only if an active-set change happens at the boundary point t_n , otherwise, it is strictly positive.

5.4. The FESD discretization

We have now introduced all extensions needed to pass from a standard RK discretization (26) to the FESD discretization for the step reformulation. With a slight abuse of notation, we collect all equations in a discrete-time system form:

$$s_1 = F_{\text{fesd}}(\mathbf{Z}), \quad (32a)$$

$$0 = G_{\text{fesd}}(\mathbf{Z}, \mathbf{h}, s_0, q, T), \quad (32b)$$

where $F_{\text{fesd}}(\mathbf{x}) = x_{N_{\text{FE}}}$ is the state transition map and $G_{\text{fesd}}(\mathbf{x}, \mathbf{h}, \mathbf{Z}, q, T)$ collects all other internal computations including all RK steps within the regarded time interval:

$$G_{\text{fesd}}(\mathbf{Z}, \mathbf{h}, s_0, q, T) := \begin{bmatrix} G_{\text{std}}(\mathbf{Z}, \mathbf{h}, s_0, q, T) \\ G_{\text{cross}}(\mathbf{A}, \mathbf{\Lambda}^p, \mathbf{\Lambda}^n) \\ G_{\text{eq}}(\mathbf{h}, \mathbf{A}, \mathbf{\Lambda}^p, \mathbf{\Lambda}^n) \\ \sum_{n=0}^{N_{\text{FE}}-1} h_n - T \end{bmatrix}. \quad (33)$$

Here, control variable q , horizon length T , and initial value s_0 are given parameters.

Remark on RK methods with $c_{n_s} \neq 1$. The extension for the case of an RK method with $c_{n_s} \neq 1$ follows similar lines as in Stewart's formulation [32]. We have that $t_n + c_{n_s} h_n < t_{n+1}$. Hence, the variables λ_{n,n_s}^p and λ_{n,n_s}^n do not correspond to the boundary values $\lambda^n(t_{n+1})$ and $\lambda^p(t_{n+1})$ anymore. We denote the true boundary points by λ_{n,n_s+1}^p and λ_{n,n_s+1}^n . They can be computed from the KKT conditions of the step reformulation LP (2). For all $n \in \{1, \dots, N_{\text{FE}} - 2\}$ we have

$$\begin{bmatrix} \psi(x_{n+1}) - \lambda_{n,n_s+1}^p + \lambda_{n,n_s+1}^n \\ \Psi(\lambda_{n,n_s+1}^n, \alpha_{n,n_s+1}) \\ \Psi(\lambda_{n,n_s+1}^p, e - \alpha_{n,n_s+1}) \end{bmatrix} = 0. \quad (34)$$

These equations are appended to the FESD equation in (33).

However, to make the switch detection work, we must update the continuity conditions for the discrete-time versions of the Lagrange multipliers and adapt the cross-complementarity conditions accordingly. For all $n = \{0, \dots, N_{\text{FE}} - 1\}$, Eq (28) is replaced by:

$$\lambda_{n,n_s+1}^p = \lambda_{n+1,0}^p, \quad \lambda_{n,n_s+1}^n = \lambda_{n+1,0}^n. \quad (35)$$

We append to the vectors $\mathbf{A}, \mathbf{\Lambda}^p$ and $\mathbf{\Lambda}^n$ the new variables $\alpha_{n,n_s+1}, \lambda_{n,n_s+1}^p$ and λ_{n,n_s+1}^n accordingly. For the whole control interval, we have in total $3(N_{\text{FE}} - 1)n_c$ new variables. It is only left to state the modified cross complementarity conditions, including the expressions' $n_s + 1$ -st points. More explicitly, the n -th component of (30) reads now for all $n \in \{0, \dots, N_{\text{FE}} - 2\}$ as

$$G_{\text{cross},n}(\mathbf{A}, \mathbf{\Lambda}^p, \mathbf{\Lambda}^n) = \sum_{k=n}^{n+1} \sum_{m=1}^{n_s} \sum_{\substack{m'=0, \\ m' \neq m}}^{n_s+1} \alpha_{k,m}^\top \lambda_{k,m'}^n + (e - \alpha_{k,m})^\top \lambda_{k,m'}^p.$$

5.5. Discretizing optimal control problem with FESD

Let us regard a nonsmooth OCP of the following form:

$$\min_{x(\cdot), u(\cdot)} \int_0^T L(x(t), u(t)) dt + R(x(T)) \quad (36a)$$

$$\text{s.t. } x_0 = s_0, \quad (36b)$$

$$\dot{x}(t) \in F(x(t), u(t), \Gamma(\psi(x(t)))) \text{, for a.a. } t \in [0, T], \quad (36c)$$

$$0 \geq G_{\text{path}}(x(t), u(t)), \quad t \in [0, T], \quad (36d)$$

$$0 \geq G_{\text{terminal}}(x(T)), \quad (36e)$$

where $L : \mathbb{R}^{n_x} \times \mathbb{R}^{n_u} \rightarrow \mathbb{R}$ is the running cost and $R : \mathbb{R}^{n_x} \rightarrow \mathbb{R}$ is the terminal cost, $s_0 \in \mathbb{R}^{n_x}$ is a given parameter. The path and terminal constraints are grouped into the functions $G_{\text{path}} : \mathbb{R}^{n_x} \times \mathbb{R}^{n_u} \rightarrow \mathbb{R}^{n_{g1}}$ and $G_{\text{terminal}} : \mathbb{R}^{n_x} \rightarrow \mathbb{R}^{n_{g2}}$, respectively.

Next, we discretize this OCP with the FESD method. Regard $N \geq 1$ control intervals of equal length, indexed by k . We take piecewise constant control discretization, where the control variables are collected $\mathbf{q} = (q_0, \dots, q_{N-1}) \in \mathbb{R}^{N n_u}$. Such a discretization is typically used in feedback control, but extensions to more elaborate control are straightforward. We equip all internal variables additionally with the index k . On every control interval k , we use the FESD discretization (32) with N_{FE} internal finite elements. The state values at the control interval boundaries are grouped in the vector $\mathbf{s} = (s_0, \dots, s_N) \in \mathbb{R}^{(N+1)n_x}$. In $\mathcal{Z} = (\mathbf{Z}_0, \dots, \mathbf{Z}_{N-1})$ we collect all internal variables and in $\mathcal{H} = (\mathbf{h}_0, \dots, \mathbf{h}_{N-1})$ all step sizes.

The discrete-time variant of (36) read as:

$$\min_{\mathbf{s}, \mathbf{q}, \mathcal{Z}, \mathcal{H}} \sum_{k=0}^{N-1} \hat{L}(s_k, \mathbf{x}_k, q_k) + R(s_N) \quad (37a)$$

$$\text{s.t. } s_0 = \bar{x}_0, \quad (37b)$$

$$s_{k+1} = F_{\text{fesd}}(\mathbf{x}_k), \quad k = 0, \dots, N-1, \quad (37c)$$

$$0 = G_{\text{fesd}}(\mathbf{x}_k, \mathbf{Z}_k, q_k), \quad k = 0, \dots, N-1, \quad (37d)$$

$$0 \geq G_{\text{ineq}}(s_k, q_k), \quad k = 0, \dots, N-1, \quad (37e)$$

$$0 \geq G_{\text{terminal}}(s_N), \quad (37f)$$

where $\hat{L} : \mathbb{R}^{n_x} \times \mathbb{R}^{(N_{\text{FE}}+1)n_s n_x} \times \mathbb{R}^{n_u} \rightarrow \mathbb{R}$ is the discretized running costs. Due to the complementarity constraints in the FESD discretization, this nonlinear program (NLP) is a mathematical program with complementarity constraints. They are degenerate NLPs since the complementarity constraints lead to the violation of standard constraint qualifications at all feasible points. In practice, they can often be efficiently solved by solving a sequence of related and relaxed NLPs within a homotopy approach. Such an approach with some of the standard reformulations [34, 7, 33] is implemented in NOSNOC. The underlying NLPs are solved via IPOPT [38] called via its CasADi interface [6].

6. Convergence theory of FESD for the step representation

In this section, we present the main convergence result of the FESD method for the step representation outlined in Eq. (32). Specifically, we show that: (1) the solutions to the FESD problem are locally isolated; (2) the solution approximations and; (3) numerical sensitivities obtained via the FESD method converge with the same order of accuracy as the underlying RK method. The proofs are similar to those used in Stewart's case in [32], hence, we will not repeat them here. The main difference is in the assumptions we make.

6.1. Main assumptions

We start by stating all assumptions. The first assumption relates to the underlying RK methods:

Assumption 9. (*Runge-Kutta method*) A Butcher tableau with the entries $a_{i,j}, b_i$ and c_i , $i, j \in \{1, \dots, n_s\}$ related to an n_s -stage Runge-Kutta (RK) method is used in the FESD (32). Moreover, we assume that:

- (a) If the same RK method is applied to the differential algebraic equation (20) on an interval $[t_a, t_b]$, with a fixed active set, it has a global accuracy of $O(h^p)$ for the differential states.
- (b) The RK equations applied to (20) have a locally isolated solution for a sufficiently small $h_n > 0$.

The second assumption concerns the existence of solutions to the FESD problem outlined in (32).

Assumption 10. (*Solution existence*) For given parameters s_0, q and T , there exists a solution to the FESD problem (32), such that for all $n \in \{0, \dots, N_{\text{FE}} - 1\}$ it holds that $h_n > 0$.

The next assumption is slightly more technical and relates to the regularity of the problem under consideration.

Assumption 11. (*Regularity*) Given the complementarity pairs $\Psi(\alpha_{n,m}, \lambda_{n,m}^n) = 0$ and $\Psi(e - \alpha_{n,m}, \lambda_{n,m}^p) = 0$, for all $n \in \{0, \dots, N_{\text{FE}} - 1\}$ there exists an $m \in \{1, \dots, n_s\}$ and $i \in \{1, \dots, n_f\}$, such that the strict complementarity property holds, i.e., $\alpha_{n,m,i} + \lambda_{n,m,i}^n > 0$ and $e - \alpha_{n,m,i} + \lambda_{n,m,i}^p > 0$. Moreover, for the RK equations (25), it holds for all $n \in \{0, \dots, N_{\text{FE}} - 1\}$, that at least one entry of the vector $\nabla_{h_n} G_{\text{rk}}(x_{n+1}, Z_n, h_n, q)$ is nonzero.

Before starting the final assumption, let us introduce some notation. We use a suitable interpolation scheme to construct a continuous-time approximation of the solution based on the stage values obtained by solving equation (32). We denote the continuous-time approximation on every finite element by $\hat{x}_n(t; h_n)$. To approximate the solution over the entire time interval $[0, T]$, we concatenate the approximations from each finite element:

$$\hat{x}_h(t) = \hat{x}_n(t; h_n) \text{ if } t \in [t_n, t_{n+1}], \quad (38)$$

where $h = \max_{n \in \{0, \dots, N_{\text{FE}} - 1\}} h_n$. The set of all grid points is defined as $\mathcal{G} = \{t_0, \dots, t_{N_{\text{FE}}}\}$. We can also use this approach to construct continuous-time representations for the algebraic variables, which we denote by $\hat{\theta}_h, \hat{\alpha}_h, \hat{\lambda}_h^n$ and $\hat{\lambda}_h^p$. The n -th switching point of the true solution is denoted by $t_{s,n}$ and one corresponding to a solution approximation by $\hat{t}_{s,n}$. Similarly, the active sets (cf. Eq. (8)) of the solution approximation are denoted by $\mathcal{I}(\hat{x}_h(t)) = \hat{\mathcal{I}}_n$, $t \in (\hat{t}_{s,n}, \hat{t}_{s,n+1})$ and the active set at switching point $\hat{t}_{s,n}$ by $\mathcal{I}(\hat{x}_h(\hat{t}_{s,n})) = \hat{\mathcal{I}}_n^0$.

Assumption 12. Let \mathcal{I}_n^0 be the active set at switching point $x(t_{s,n})$ of true solution and $\hat{\mathcal{I}}_n^0$ the active set at the switching point $\hat{x}(\hat{t}_{s,n})$ a solution approximation. If $\hat{t}_{s,n}$ is sufficiently close to $t_{s,n}$ and $\mathcal{I}_n^0 = \hat{\mathcal{I}}_n^0$, then $\mathcal{I}_{n+1} = \hat{\mathcal{I}}_{n+1}$. Furthermore, if there are several possible new active sets, they are identical for both the true solution and its approximation.

6.2. Solutions of the FESD problem are locally isolated

In this section, we present a theorem on the regularity of solutions to the FESD problem (32). For simplicity, we focus on the case where $c_{n_s} = 1$ and explain how the theorem can be extended to other cases. Additionally, to improve readability, we restate the FESD problem.

$$G_{\text{fesd}}(\mathbf{Z}, \mathbf{h}, s_0, q, T) := \begin{bmatrix} G_{\text{std}}(\mathbf{Z}, \mathbf{h}, s_0, q, T) \\ G_{\text{cross}}(\mathbf{A}, \mathbf{\Lambda}^p, \mathbf{\Lambda}^n) \\ G_{\text{eq}}(\mathbf{h}, \mathbf{A}, \mathbf{\Lambda}^p, \mathbf{\Lambda}^n) \\ \sum_{n=0}^{N_{\text{FE}}-1} h_n - T \end{bmatrix}. \quad (39)$$

Furthermore, we provide a summary of the dimensions of all key functions and variables:

- Degrees of freedom: $\mathbf{Z} = (\mathbf{x}, \mathbf{V}, \boldsymbol{\Theta}, \mathbf{A}, \boldsymbol{\Lambda}^p, \boldsymbol{\Lambda}^n)$ and \mathbf{h} .
- Total number of degrees of freedom: $N_{\text{FE}} + n_{\mathbf{Z}}$, where $n_{\mathbf{Z}} = (N_{\text{FE}} + 1)n_x + N_{\text{FE}}n_s n_x + n_\theta + 3n_\alpha$.
- Dimension of $\boldsymbol{\Theta}$: $n_\theta = N_{\text{FE}}n_s n_f$.
- Dimension of $\mathbf{A}, \boldsymbol{\Lambda}^p, \boldsymbol{\Lambda}^n$: $n_\alpha = N_{\text{FE}}n_s n_c$.
- Parameters: $(s_0, q, T) \in \mathbb{R}^{n_x + n_u + 1}$,
- Standard RK equations: $G_{\text{std}} : \mathbb{R}^{n_{\mathbf{Z}}} \times \mathbb{R}^{N_{\text{FE}}} \times \mathbb{R}^{n_x} \times \mathbb{R}^{n_u} \times \mathbb{R} \rightarrow \mathbb{R}^{n_{\mathbf{Z}}}$,
- Cross complementarity: $G_{\text{cross}} : \mathbb{R}^{n_\alpha} \times \mathbb{R}^{n_\alpha} \times \mathbb{R}^{n_\alpha} \rightarrow \mathbb{R}^{N_{\text{FE}} - 1}$,
- Step equilibration: $G_{\text{eq}} : \mathbb{R}^{N_{\text{FE}}} \times \mathbb{R}^{n_\alpha} \times \mathbb{R}^{n_\alpha} \times \mathbb{R}^{n_\alpha} \rightarrow \mathbb{R}^{N_{\text{FE}} - 1}$ and
- FESD equations: $G_{\text{fesd}} : \mathbb{R}^{n_{\mathbf{Z}}} \times \mathbb{R}^{N_{\text{FE}}} \times \mathbb{R}^{n_x} \times \mathbb{R}^{n_u} \times \mathbb{R} \rightarrow \mathbb{R}^{n_{\mathbf{Z}} + 2N_{\text{FE}} - 1}$.

The vectors $s_0 \in \mathbb{R}^{n_x}$, $q \in \mathbb{R}^{n_u}$ and $T \in \mathbb{R}$ are given parameters. As a result, the system of equations (39) has a total of $n_{\mathbf{Z}} + N_{\text{FE}}$ unknowns and $n_{\mathbf{Z}} + 2N_{\text{FE}} - 1$ equations, which means it is always over-determined. Similar to Stewart's representation, we have that for a given active set $N_{\text{FE}} - 1$ equations in (39) are implicitly satisfied. This results in a reduced system with $n_{\mathbf{Z}} + N_{\text{FE}}$ equations, which we can show to be well-posed. However, the specific active set at the solution is not known in advance, so when searching for a solution, we must consider all equations in (39).

Theorem 13. *Suppose that Assumptions 9, 10 and 11 hold. Let s_0 , q_0 and T be some fixed parameters such that $G_{\text{fesd}}(\mathbf{Z}^*, \mathbf{h}^*, s_0, q, T) = 0$ in Eq. (39). Let $P^* \subseteq \mathbb{R}^{n_x} \times \mathbb{R}^{n_u} \times \mathbb{R}$ be the set of all parameters $(\hat{s}_0, \hat{q}, \hat{T})$ such that $\mathbf{Z} \in \mathbb{R}^{n_{\mathbf{Z}}}$, which is the solution of $G_{\text{fesd}}(\mathbf{Z}, \mathbf{h}, \hat{s}_0, \hat{q}, \hat{T}) = 0$, has the same active set as \mathbf{Z}^* . Additionally, suppose that $G_{\text{fesd}}(\cdot)$ is continuously differentiable in s_0, q and T for all $(s_0, q, T) \in P^*$. Then there exists a neighborhood $P \subseteq P^*$ of (s_0, q_0, T) such that there exist continuously differentiable single valued functions $\mathbf{Z}^* : P \rightarrow \mathbb{R}^{n_{\mathbf{Z}}}$ and $\mathbf{h}^* : P \rightarrow \mathbb{R}^{N_{\text{FE}}}$.*

Proof. The proof follows similar lines as the proof of [32, Theorem 14] and we omit it for brevity. \square

6.2.1. Extension for the case of $c_{n_s} \neq 1$

If $c_{n_s} \neq 1$, then the right boundary point is not a RK-stage point. We solve (34) to obtain the boundary points. If some $\psi_j(x_{n+1}) = 0$, then $\alpha_{n, n_s+1, j}$ is not uniquely determined. However, we only need the right boundary points of the Lagrange multipliers in the cross-complementarity conditions. Therefore, we can discard $\alpha_{n, n_s+1, j}$ and compute only the multipliers. This simplifies (34) to:

$$\begin{aligned} \psi(x_{n+1}) - \lambda_{n, n_s+1}^p + \lambda_{n, n_s+1}^n &= 0, \\ \lambda_{n, n_s+1}^n &\geq 0, \\ \lambda_{n, n_s+1}^p &\geq 0. \end{aligned}$$

These conditions are added to the FESD equations in (32). However, we have $2n_c$ unknowns and n_c equalities and $2n_c$ inequalities for a given x_{n+1} . Next, we show that we still obtain a well-posed problem for a given active set. Recall that $\mathcal{C} = \{1, \dots, n_c\}$. We define the following index sets for all $n \in \{0, \dots, N_{\text{FE}} - 1\}$:

$$\begin{aligned} \mathcal{C}_n^{\text{pn}} &= \{j \in \mathcal{C} \mid \lambda_{n, n_s+1, j}^p = \lambda_{n, n_s+1, j}^n = 0\}, \\ \mathcal{C}_n^{\text{p}} &= \{j \in \mathcal{C} \mid \lambda_{n, n_s+1, j}^p = 0, \lambda_{n, n_s+1, j}^n > 0\}, \\ \mathcal{C}_n^{\text{n}} &= \{j \in \mathcal{C} \mid \lambda_{n, n_s+1, j}^n = 0, \lambda_{n, n_s+1, j}^p > 0\}. \end{aligned}$$

Note that due to the complementarity conditions, there is no $j \in \mathcal{C}$ such that $\lambda_{n,m,j}^n > 0$ and $\lambda_{n,m,j}^p > 0$ for $m \in \{1, \dots, n_s\}$. From the cross complementarity conditions, it follows that the same is true for $m = n_s + 1$. Consequently, we have that $\mathcal{C} = \mathcal{C}_n^{\text{pn}} \cup \mathcal{C}_n^n \cup \mathcal{C}_n^p$. Therefore, in a solution we have

$$\lambda_{n,n_s+1}^n = 0, \quad j \in \mathcal{C}_n^{\text{pn}} \cup \mathcal{C}_n^p, \quad (40a)$$

$$\lambda_{n,n_s+1}^p = 0, \quad j \in \mathcal{C}_n^{\text{pn}} \cup \mathcal{C}_n^n, \quad (40b)$$

$$\psi(x_{n+1}) + \lambda_{n,n_s+1}^n = 0, \quad j \in \mathcal{C}_n^p, \quad (40c)$$

$$\psi(x_{n+1}) - \lambda_{n,n_s+1}^p = 0, \quad j \in \mathcal{C}_n^n. \quad (40d)$$

In total, we are left with $2(|\mathcal{C}_n^{\text{pn}}| + |\mathcal{C}_n^p| + |\mathcal{C}_n^n|) = 2n_c$ binding equations. The new variables are determined by the square linear system (40). Hence, it is straightforward to extend Theorem 13 to the case of $c_{n_s} \neq 1$.

6.3. Convergence of the FESD method

We proceed by stating the results of the convergence of the FESD method. We show that under suitable assumptions, the sequence of approximations $\hat{x}_h(\cdot)$ generated by the FESD method converges to a solution of (6). In particular, the FESD method has the same order as the underlying RK method for smooth ODE.

Theorem 14. *Let $x(\cdot)$ be a solution of (6) with finitely many active set changes for $t \in [0, T]$ with $x(0) = x_0$. Suppose the following is true:*

(a) *The Assumptions 5 and 12 are satisfied.*

(b) *The Assumptions 9, 10 and 11 hold for the FESD problem (32).*

Then $x(\cdot)$ is a limit point of the sequence of approximations $\hat{x}_h(\cdot)$, defined in Eq. (38) as $h \downarrow 0$. Moreover, for sufficiently small $h > 0$, the solution of (32) generates a solution approximation $\hat{x}_h(t)$ on $[0, T]$ such that:

$$|\hat{t}_{s,n} - t_{s,n}| = O(h^p) \text{ for every } n \in \{0, \dots, N_{\text{sw}}\}, \quad (41a)$$

$$\|\hat{x}_h(t) - x(t)\| = O(h^p), \text{ for all } t \in \mathcal{G}. \quad (41b)$$

Proof. The proof follows similar lines as the proof of [32, Theorem 16]. The primary distinction lies in the prediction of new active sets. In [32, Theorem 16], we use [32, Assumption 8] to be able to apply [35, Lemma A.2] and demonstrate that both the approximation and the exact solution share the same active set in the vicinity of a switching point. In this theorem, the assertion emerges directly from Assumption 12. \square

6.4. Convergence of discrete-time sensitivities

This section concludes by demonstrating that the numerical sensitivities obtained using the FESD method for the step reformulation converge to the correct values with a high order of accuracy. We remind the reader that numerical sensitivities of standard time-stepping methods, e.g. (26), do not converge to the correct values, no matter how small the step size becomes [37]. The convergence of the sensitivities is crucial for the success of direct optimal control methods [27].

Before stating the result, we assume the time derivatives of the solution approximation \hat{x}_h converge accordingly. This assumption extends Assumption 9 and allows us to consider a wide range of RK methods.

Assumption 15. *(RK derivatives) Regard the RK methods from Assumption 9 applied to the differential algebraic equations (20). The derivatives of the numerical approximation for the same RK method converge with order $1 \leq q \leq p$, i.e., $\|\hat{\dot{x}}_h(t) - \dot{x}(t)\| = O(h^q)$, $t \in \mathcal{G}$.*

We remind the reader that for collocation-based implicit RK methods for ODE in general it holds that $q = p - 1$ [21, Theorem 7.10].

Theorem 16 (Convergence to exact sensitivities). *Suppose the assumptions of Theorem 14 and Assumption 15 hold. Assume that a single active-set change happens at time $t_{s,n}$, i.e., $||\mathcal{I}_n| - |\mathcal{I}_{n+1}|| \leq 1, n \in \{0, \dots, N_{sw}\}$. Then for $h \downarrow 0$ it holds that $\frac{\partial \hat{x}_h(t, x_0)}{\partial x_0} \rightarrow \frac{\partial x(t, x_0)}{\partial x_0}$ with the convergence rate*

$$\left\| \frac{\partial \hat{x}_h(t, x_0)}{\partial x_0} - \frac{\partial x(t, x_0)}{\partial x_0} \right\| = O(h^q), \text{ for all } t \in \mathcal{G}. \quad (42)$$

Proof. The proof is essentially the same as the proof of [32, Theorem 18], one has only to replace the local switching functions $\psi_{i,j}(x)$ by an appropriate switching function $\psi_k(x)$. \square

7. Numerical examples

In this section, we show a simulation example with a gene regulatory network model, which is described by a DI of the form (5). The model is not a Filippov system, but a more general DI. We show empirically that the FESD method has the same accuracy order that the underlying Runge-Kutta method has for smooth ODEs. More numerical examples with FESD for the step reformulation can be found in [30]. In the mentioned reference, we generated integration order plots for a Filippov system and confirmed empirically the results of Theorem 14. Moreover, we regarded an optimal control example of a simple one-legged robot. In this example, we compared Stewart's reformulation to the step reformulation. Here, we carry out a similar experiment, but with a more complicated example. We regard a planar two-link monopod that must reach a certain goal in the horizontal direction. We compare the step reformulation and Stewart's reformulation in terms of total computational time and cost-per-iteration.

7.1. Gene regulatory networks

We regard the IRMA example, a synthetic network composed of five genes, originally proposed in [11]. This example is inspired by [4], which includes more examples with step function switches that are implemented in `nosnoc` [2].

IRMA model. In Figure 4, we reproduced the state trajectories from [4, Fig. 11]. Additionally, the vertical lines show the switching times of the selection variables α_i . The states of this system are the protein concentrations of Gal4, Swi5, Ash1, Cbf1, and Gal80, which are denoted by x_1, \dots, x_5 . There are seven switching functions, which are defined by the states crossing certain thresholds, which are plotted as horizontal lines in Figure 4. Specifically, the switching functions are

$$\psi(x) = (x_1 - 0.01, x_2 - 0.01, x_2 - 0.06, x_2 - 0.08, x_3 - 0.035, x_4 - 0.04, x_5 - 0.01).$$

Note that Swi5 (x_2) has three threshold values. The continuous-time dynamics of the system are given by

$$\dot{x}_1 \in -p_1 x_1 + \kappa_1^1 + \kappa_1^2 \gamma(\psi_6(x)), \quad (43a)$$

$$\dot{x}_2 \in -p_2 x_2 + \kappa_2^1 + \kappa_2^2 \gamma(\psi_1(x))(1 - u) \gamma(\psi_7(x)), \quad (43b)$$

$$\dot{x}_3 \in -p_3 x_3 + \kappa_3^1 + \kappa_3^2 \gamma(\psi_3(x)), \quad (43c)$$

$$\dot{x}_4 \in -p_4 x_4 + \kappa_4^1 + \kappa_4^2 \gamma(\psi_2(x))(1 - \gamma(\psi_5(x))), \quad (43d)$$

$$\dot{x}_5 \in -p_5 x_5 + \kappa_5^1 + \kappa_5^2 \gamma(\psi_4(x)). \quad (43e)$$

Note that $u \in \{0, 1\}$ is an external input, which is set to $u = 1$ in the scenario considered here. The initial state is given by $x_0 = (0.011, 0.09, 0.04, 0.05, 0.015)$. The parameter values are given as

$$\begin{aligned} p &= (0.05, 0.04, 0.05, 0.02, 0.6), \\ \kappa^1 &= (1.1 \cdot 10^{-4}, 3 \cdot 10^{-4}, 6 \cdot 10^{-4}, 5 \cdot 10^{-4}, 7.5 \cdot 10^{-4}) \\ \kappa^2 &= (9 \cdot 10^{-4}, 0.15, 0.018, 0.03, 0.015). \end{aligned}$$

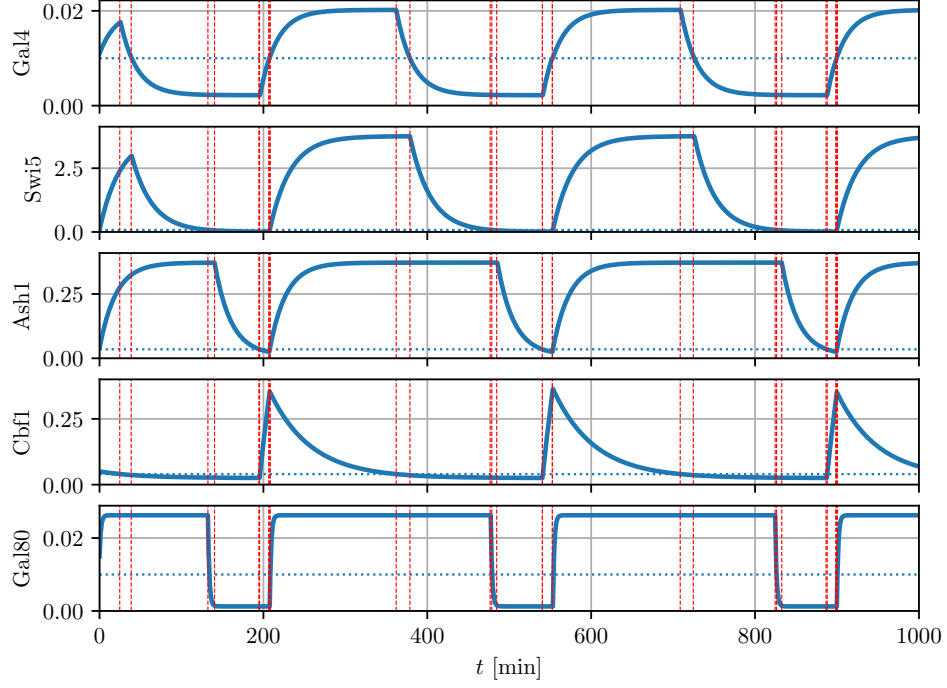


Figure 4: State trajectory of the IRMA example with red dotted vertical lines indicating the switches.

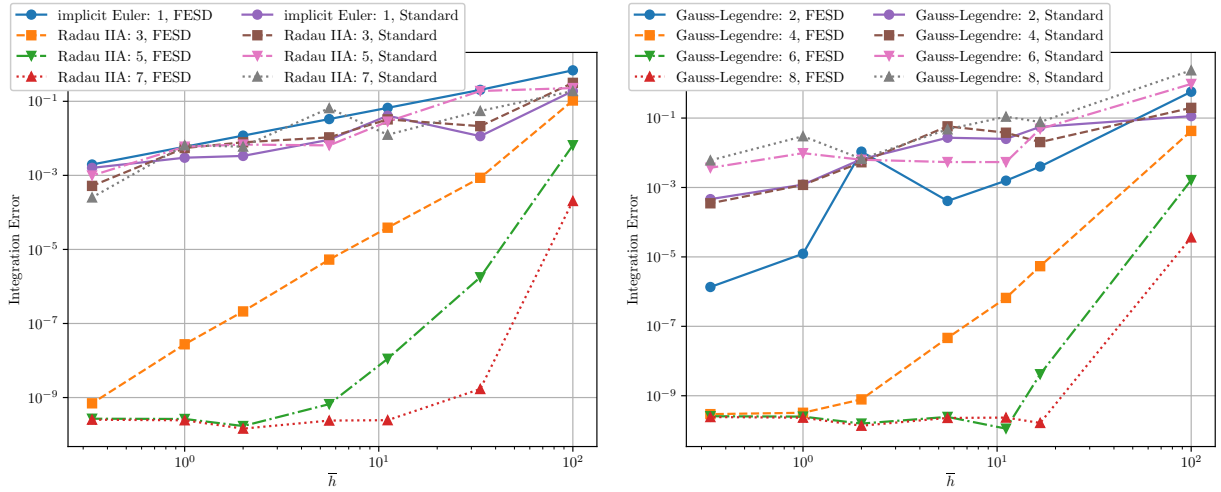


Figure 5: Accuracy vs. step size: Simulation of first 100 minutes of the trajectory in Figure 4 with different RK schemes and step sizes.

Integration order experiment. To showcase that the FESD step reformulation preserves the integration order of the underlying Runge-Kutta method, we simulate the first 100 minutes of the trajectory depicted in Figure 4. This time interval contains exactly two switches. We use $N_{\text{FE}} = 3$, to capture those switches even with a single FESD step. We plot the integration error over the average step size $\bar{h} = T_{\text{sim}}/N_{\text{sim}}N_{\text{FE}}$, where N_{sim} is the total number of simulation steps. The results are summarized in Figure 5 for FESD with underlying Radau IIA of orders 1, 3, 5, and 7, and Gauss-Legendre methods of orders 2, 4, 6, and 8. It can be seen that the FESD step formulation preserves the integration order of the underlying Runge-Kutta method, while with the standard approach, using methods that typically have higher order integration accuracy degrade to order one without FESD. This experiment shows, that if a feasible solution is found the integration order of the underlying Runge-Kutta method is preserved. The implementation of the example is publicly available³.

7.2. Optimal control example with state jumps

Now we further investigate the use of FESD for the step reformulation by applying it to an optimal control problem. We regard the problem of synthesizing dynamic motions of the two-link *Capler* robot with state jumps and friction [12]. Systems with state jumps, do not directly fit the form of ODEs with set-valued step functions (5). However, using the time-freezing reformulation we can transform the system with state jumps into a PSS of the form of (6) [31] and used the methods developed in this paper.

The monopod's configuration is described by four degrees of freedom $q = (q_x, q_z, \phi_{\text{knee}}, \phi_{\text{hip}})$, where (q_x, q_z) are the coordinates of the monopod's base at the hip and $\phi_{\text{knee}}, \phi_{\text{hip}}$ are the angles of the hip and knee. The robot is actuated by two direct-drive motors at the hip and knee joints. The control variables are the torques of these motors $u(t) = (u_{\text{knee}}(t), u_{\text{hip}}(t))$. Denote by $p_{\text{foot}}(q) = (p_{\text{foot},x}(q), p_{\text{foot},z}(q))$ and $p_{\text{knee}}(q) = (p_{\text{knee},x}(q), p_{\text{knee},z}(q))$ the kinematic position of the robot's foot and knee, respectively. We model a single contact point, the tip of the robot's foot touching the ground, which is expressed via the unilateral constraint

$$f_c(q) = p_{\text{foot},z}(q) \geq 0.$$

Moreover, we denote the expression summarizing the Coriolis, control, and gravitational forces by $f_v(q, u)$, the inertia matrix by $M(q)$, the normal contact Jacobian by $J_n(q) \in \mathbb{R}^{n_q}$, and the contact tangent by $J_t(q) \in \mathbb{R}^{n_q}$. The detailed derivation of all mentioned functions, i.e., the model equations, kinematic expressions, and all parameters for the robot can be found in [18, Appendix A].

After the time-freezing reformulation, the PSS state consists of $x(\tau) = (q(\tau), v(\tau), t(\tau)) \in \mathbb{R}^9$, where $q(\tau)$ being the position, $v(\tau)$ the velocity, $t(\tau)$ is a clock state needed for the time-freezing reformulation and τ is the time of the ODE, cf. [31]. For the time-freezing PSS, we have in total tree switching functions: the gap function, as well as the normal and tangential contact velocities [31]:

$$\psi(x) = (f_c(q), J_n(q)^\top v, J_t(q)^\top v).$$

This allows a definition of eight basis sets via the sign matrix (cf. Definition 2):

$$S = \begin{bmatrix} 1 & 1 & 1 \\ 1 & 1 & -1 \\ 1 & -1 & 1 \\ 1 & -1 & -1 \\ -1 & 1 & 1 \\ -1 & 1 & -1 \\ -1 & -1 & 1 \\ -1 & -1 & -1 \end{bmatrix}$$

³https://github.com/FreyJo/nosnoc_py/blob/main/examples/Acary2014/irma_integration_order_experiment.py

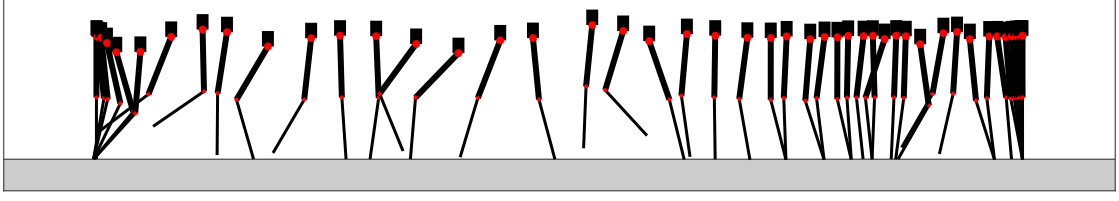


Figure 6: Illustration of several frames of the solution of the discretized OCP.

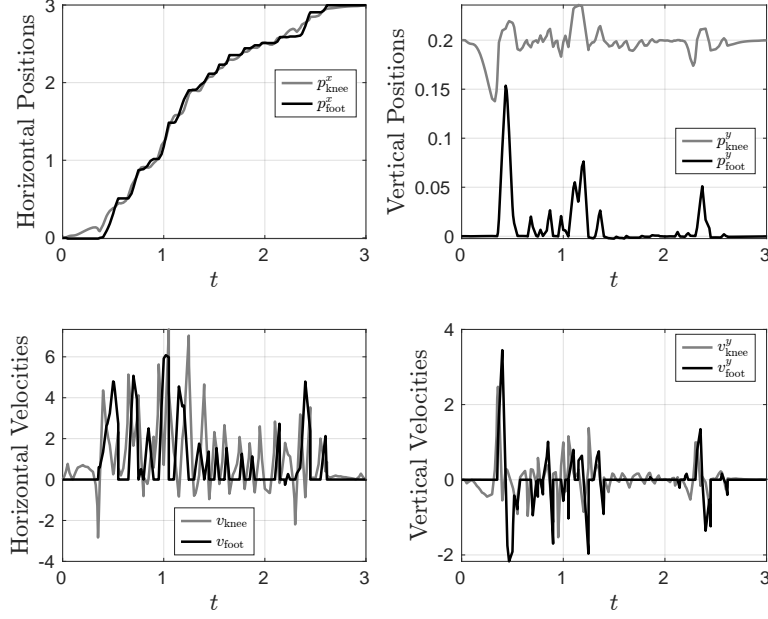


Figure 7: The monopod's vertical and horizontal positions (top plots), and velocities (bottom plots).

However, the time-freezing PSS has only three regions, where the first one consists of the union of the first six basis sets, and the other two match the two remaining basis sets. In equations this reads as

$$\begin{aligned} R_1 &= \cup_{i=1}^6 \tilde{R}_i = \{x \in \mathbb{R}^{n_x} \mid f_c(q) > 0\} \cup \{x \in \mathbb{R}^{n_x} \mid f_c(q) < 0, J_n(q)^\top v > 0\}, \\ R_2 &= \tilde{R}_7 = \{x \in \mathbb{R}^{n_x} \mid f_c(q) < 0, J_n(q)^\top v < 0, J_t(q)^\top v > 0\}, \\ R_3 &= \tilde{R}_8 = \{x \in \mathbb{R}^{n_x} \mid f_c(q) < 0, J_n(q)^\top v < 0, J_t(q)^\top v < 0\}. \end{aligned}$$

In region R_1 , we define the unconstrained (free flight) dynamics of the monopod, and in regions, R_2 and R_3 , auxiliary ODEs that mimic state jumps in normal and tangential directions due to frictional impacts:

$$\begin{aligned} f_1(x, u) &= (q, M(q)^{-1} f_v(q, u), 1), \\ f_2(x) &= (\mathbf{0}_{4,1}, M(q)^{-1} (J_n(q) - J_t(q)\mu) a_n, 0), \\ f_3(x) &= (\mathbf{0}_{4,1}, M(q)^{-1} (J_n(q) + J_t(q)\mu) a_n, 0). \end{aligned}$$

Here, $a_n = 200$ is the auxiliary ODE's constant [31] and the coefficient of friction is $\mu = 0.8$. Observe that the clock state dynamics are $\frac{dt}{d\tau} = 1$ in R_1 , and $\frac{dt}{d\tau} = 0$ in R_2 and R_3 . A solution trajectory of a PSS is continuous in time. By taking the pieces of the trajectory where $\frac{dt}{d\tau} > 0$, we recover the solution of the original system with state jumps [31].

It follows from the discussion in Section 4, that with the step reformulation, we have $\theta \in \mathbb{R}^3$. Since we have $n_\psi = 3$, the step DCS (13) for our examples has three complementarity constraints and six equality

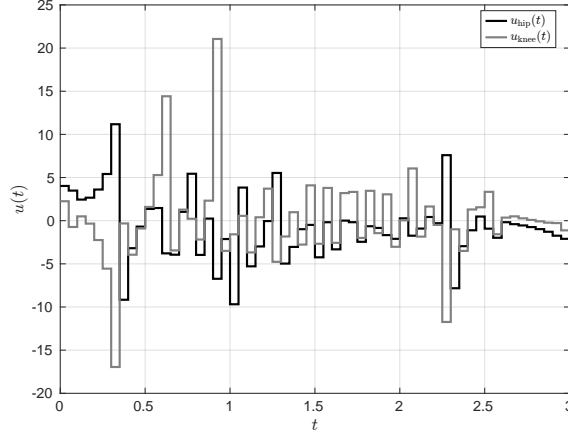


Figure 8: The optimal controls for the example of $N = 60$ control stages.

constraints. For Stewart’s reformulation, we cannot exploit the union of basis sets but must define eight regions, which are equal to the basis sets. However, the first six regions are equipped with $f_1(x, u)$ and the remaining two with $f_2(x)$ and $f_3(x)$. In this case, we have $\theta \in \mathbb{R}^8$, eight complementarity constraints and nine equality constraints in the DCS (19). Using the step reformulation for this problem allows us to reduce the number of regions we need to define from eight to only three.

To compare the performances of the two reformulations, we run an experiment in which the robot reaches a target position $q_{\text{target}} = (3, 0.4, 0, 0)$ with zero velocity $v_{\text{target}} = \mathbf{0}_{4,1}$ in $T = 3.0$ seconds. The initial state is $x(0) = (0, 0.4, 0, 0, 0, 0, 0, 0, 0)$. Given a reference $x^{\text{ref}}(t)$, which is spline interpolation between the initial and final position, and includes two jumps, we define the least-squares objective with the running and terminal costs:

$$\begin{aligned} L(x(\tau), u(\tau)) &= (x(\tau) - x^{\text{ref}}(\tau))^{\top} Q (x(\tau) - x^{\text{ref}}(\tau)) + \rho_u u(\tau)^{\top} u(\tau), \\ R(x(T)) &= (x(T) - x^{\text{ref}}(T))^{\top} Q_T (x(T) - x^{\text{ref}}(T)), \end{aligned}$$

where the weight matrices are $Q = \text{diag}(1, 1, 10, 1, 10^{-6}, 10^{-6}, 10^{-6}, 10^{-6}, 0)$, $\rho_u = 0.01$, and $Q_T = \text{diag}(10^3, 10^3, 10^3, 10^3, 10, 10, 10, 10, 0)$. We define the state and control bound constraints:

$$\begin{aligned} x_{\text{lb}} &\leq x(\tau) \leq x_{\text{ub}}, \\ u_{\text{lb}} &\leq u(\tau) \leq u_{\text{ub}}, \end{aligned}$$

where $x_{\text{ub}} = (3.5, 10, \pi, \pi, 100, 100, 100, 100, \infty)$, $x_{\text{lb}} = (-0.5, 0, -\pi, -\pi, -100, -100, -100, -100, -\infty)$, $u_{\text{ub}} = (100, 100)$, and $u_{\text{lb}} = -u_{\text{ub}}$.

Collecting all the above, we can define an OCP of the form of (36), which we discretized with the FESD Radau IIA scheme of order 3 ($n_s = 2$), with $N_{\text{FE}} = 3$ finite elements on every control interval. This OCP is discretized and solved with `nosnoc` in a homotopy loop with `IPOPT` [38]. Figure 6 illustrates several frames of an example solution ($N = 60$). Figure 7 shows the relevant vertical and horizontal positions and velocities, and Figure 8 shows the optimal controls.

Next, we solve this OCP for different values N (number of control intervals) from 30 to 90 in increments of 10 and compare FESD for the step reformulation (this paper) to FESD derived for Stewart’s reformulation [32]. We compare the CPU time per NLP iteration and total CPU time for both approaches in Figure 9. As expected, due to the smaller number of variables and constraints, the step reformulation leads to faster NLP iterations than the Stewart reformulation. In our experiments, we tried different linear solvers from the HSL library [24]. The linear solver choice had a particularly strong influence on performance for both the Stewart and Step implementations. After evaluation, we selected the best linear solver for each one, which is `ma27` for Stewart reformulation and `ma97` for the step reformulation. In particular, for the Stewart reformulation, we observed that `ma97`, by all accounts the superior algorithm, would fail at some stages. We can see the linear algebra costs increase significantly, for $N > 60$, as the linear solvers need more time

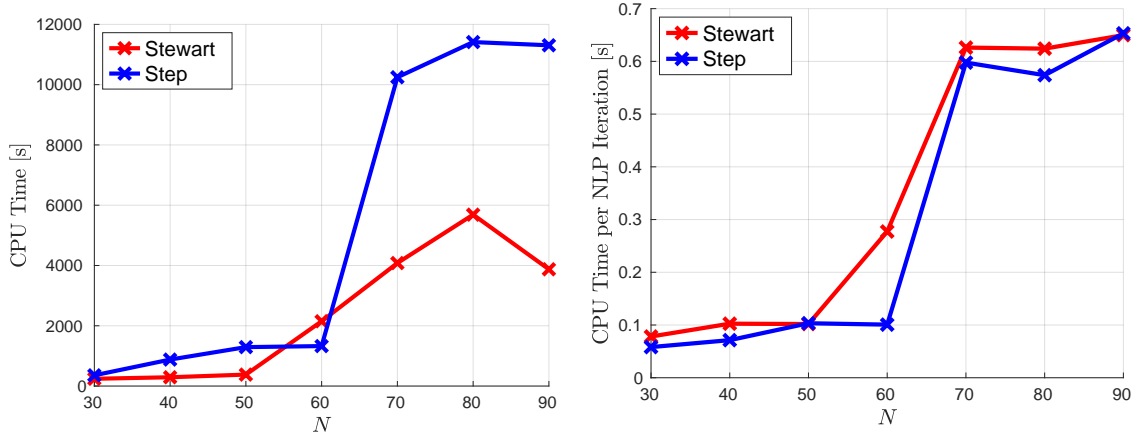


Figure 9: The total CPU time of the homotopy loop for different N (left plot) and the CPU time per NLP solver iteration (right plot).

to factorize larger systems. The total computation time is influenced by many several factors: homotopy algorithm, initialization, NLP solver performance, linear algebra solver, etc., and as such shows a less clear trend. In this example, Stewart’s reformulation achievea consistently lower computation times despite a higher cost per iteration. On the other hand, in our experiments in [30], we had a similar setting where the Step reformulation led to lower total computational times. We can conclude that which reformulation is the better, depends strongly on the example and the chosen optimization algorithm parameters.

8. Conclusion

This paper extends the Finite Elements with Switch Detection to nonsmooth dynamical systems with set-valued step functions, such as Filippov systems, which are a prominent subclass of the regarded systems. Using the KKT condition of a linear program, we derive from the initial nonsmooth systems an equivalent Dynamic Complementarity System (DCS). We exploit the continuity of the Lagrange multipliers and derive a discretization method that detects exactly the nonsmooth transition in time. Compared to Stewart’s reformulation used in [32], the step reformulation allows for a more compact definition of regions if some of them do not depend on all switching functions or if they are defined as the unions, intersection, or differences of some sets. This results in fewer algebraic variables in the DCS. Furthermore, the step-representation is suitable to represent more general systems than Filippov systems, e.g., Aizerman–Pyatnitskii inclusions [4, 17]. The comparison of the new FESD method to FESD for Stewart’s reformulation on an optimal control example shows that the new approach has a lower cost per iteration, but might have a longer total computation time for some problem instances. However, the total computation time depends on many factors, e.g., the specific problem at hand, the initial guess, the homotopy loop parameters, etc. For example, in [30], FESD for the step reformulation had both lower cost per iteration and total CPU time than FESD for Stewart’s reformulation.

References

- [1] NOSNOC. <https://github.com/nurkanovic/nosnoc>, 2022.
- [2] nosnoc.py. https://github.com/FreyJo/nosnoc_py, 2022.
- [3] Vincent Acary and Bernard Brogliato. *Numerical methods for nonsmooth dynamical systems: applications in mechanics and electronics*. Springer Science & Business Media, 2008.
- [4] Vincent Acary, Hidde De Jong, and Bernard Brogliato. Numerical simulation of piecewise-linear models of gene regulatory networks using complementarity systems. *Physica D: Nonlinear Phenomena*, 269:103–119, 2014.
- [5] J. Albersmeyer and M. Diehl. The lifted Newton method and its application in optimization. *SIAM Journal on Optimization*, 20(3):1655–1684, 2010.
- [6] J. A. E. Andersson, J. Gillis, G. Horn, J. B. Rawlings, and M. Diehl. CasADi – a software framework for nonlinear optimization and optimal control. *Mathematical Programming Computation*, 11(1):1–36, 2019.

- [7] Mihai Anitescu, Paul Tseng, and Stephen J Wright. Elastic-mode algorithms for mathematical programs with equilibrium constraints: global convergence and stationarity properties. *Mathematical programming*, 110(2):337–371, 2007.
- [8] Brian T Baumrucker and Lorenz T Biegler. Mpec strategies for optimization of a class of hybrid dynamic systems. *Journal of Process Control*, 19(8):1248–1256, 2009.
- [9] A. Bemporad and M. Morari. Control of systems integrating logic, dynamics, and constraints. *Automatica*, 35(3):407–427, 1999.
- [10] Mario Bernardo, Chris Budd, Alan Richard Champneys, and Piotr Kowalczyk. *Piecewise-smooth dynamical systems: theory and applications*, volume 163. Springer Science & Business Media, 2008.
- [11] Irene Cantone, Lucia Marucci, Francesco Iorio, Maria Aurelia Ricci, Vincenzo Belcastro, Mukesh Bansal, Stefania Santini, Mario di Bernardo, Diego di Bernardo, and Maria Pia Cosma. A yeast synthetic network for in vivo assessment of reverse-engineering and modeling approaches. *Cell*, 137(1):172–181, 2009.
- [12] Jan Carius, René Ranftl, Vladlen Koltun, and Marco Hutter. Trajectory optimization with implicit hard contacts. *IEEE Robotics and Automation Letters*, 3(4):3316–3323, 2018.
- [13] P. Cortes, M.P. Kazmierkowski, R.M. Kennel, D.E. Quevedo, and J. Rodriguez. Predictive control in power electronics and drives. *IEEE Transactions on Industrial Electronics*, 55(12):4312–4324, 2008.
- [14] Luca Dieci and Luciano Lopez. Sliding motion in filippov differential systems: theoretical results and a computational approach. *SIAM Journal on Numerical Analysis*, 47(3):2023–2051, 2009.
- [15] Luca Dieci and Luciano Lopez. Sliding motion on discontinuity surfaces of high co-dimension. a construction for selecting a filippov vector field. *Numerische Mathematik*, 117(4):779–811, 2011.
- [16] F. Facchinei and J.-S. Pang. *Finite-dimensional variational inequalities and complementarity problems*, volume 1-2. Springer-Verlag, 2003.
- [17] AF Filippov. *Differential Equations with Discontinuous Righthand Sides: Control Systems*, volume 18. Springer Science & Business Media, 1988.
- [18] Christian Gehring. Operational space control of single legged hopping. Master’s thesis, Eidgenössische Technische Hochschule Zürich, Autonomous Systems Lab, 2011.
- [19] Nicola Guglielmi and Ernst Hairer. An efficient algorithm for solving piecewise-smooth dynamical systems. *Numerical Algorithms*, 89(3):1311–1334, 2022.
- [20] Lei Guo and Jane J Ye. Necessary optimality conditions for optimal control problems with equilibrium constraints. *SIAM Journal on Control and Optimization*, 54(5):2710–2733, 2016.
- [21] E. Hairer, S.P. Nørsett, and G. Wanner. *Solving Ordinary Differential Equations I*. Springer Series in Computational Mathematics. Springer, Berlin, 2nd edition, 1993.
- [22] E. Hairer and G. Wanner. *Solving Ordinary Differential Equations II – Stiff and Differential-Algebraic Problems*. Springer, Berlin Heidelberg, 2nd edition, 1991.
- [23] Mathew Halm and Michael Posa. Set-valued rigid body dynamics for simultaneous frictional impact. *arXiv preprint arXiv:2103.15714*, 2021.
- [24] HSL. A collection of Fortran codes for large scale scientific computation., 2011.
- [25] Anna Machina and Arcady Ponosov. Filippov solutions in the analysis of piecewise linear models describing gene regulatory networks. *Nonlinear Analysis: Theory, Methods & Applications*, 74(3):882–900, 2011.
- [26] Armin Nurkanović, Sebastian Albrecht, Bernard Brogliato, and Moritz Diehl. The Time-Freezing Reformulation for Numerical Optimal Control of Complementarity Lagrangian Systems with State Jumps. *arXiv preprint*, 2021.
- [27] Armin Nurkanović, Sebastian Albrecht, and Moritz Diehl. Limits of MPCC Formulations in Direct Optimal Control with Nonsmooth Differential Equations. In *2020 European Control Conference (ECC)*, pages 2015–2020, 2020.
- [28] Armin Nurkanović and Moritz Diehl. Continuous optimization for control of hybrid systems with hysteresis via time-freezing. *IEEE Control Systems Letters*, 2022.
- [29] Armin Nurkanović and Moritz Diehl. NOSNOC: A software package for numerical optimal control of nonsmooth systems. *IEEE Control Systems Letters*, 2022.
- [30] Armin Nurkanović, Jonathan Frey, Anton Pozharskiy, and Moritz Diehl. Finite elements with switched detection for direct optimal control of nonsmooth systems with set-valued step functions. *arXiv preprint arXiv:2303.18066*, 2023.
- [31] Armin Nurkanović, Tommaso Sartor, Sebastian Albrecht, and Moritz Diehl. A Time-Freezing Approach for Numerical Optimal Control of Nonsmooth Differential Equations with State Jumps. *IEEE Control Systems Letters*, 5(2):439–444, 2021.
- [32] Armin Nurkanović, Mario Sperl, Sebastian Albrecht, and Moritz Diehl. Finite Elements with Switch Detection for Direct Optimal Control of Nonsmooth Systems. 2022.
- [33] Daniel Ralph and Stephen J. Wright. Some properties of regularization and penalization schemes for mpecs. *Optimization Methods and Software*, 19(5):527–556, 2004.
- [34] Stefan Scholtes. Convergence properties of a regularization scheme for mathematical programs with complementarity constraints. *SIAM Journal on Optimization*, 11(4):918–936, 2001.
- [35] David Stewart. A high accuracy method for solving odes with discontinuous right-hand side. *Numerische Mathematik*, 58(1):299–328, 1990.
- [36] David E Stewart. A numerical method for friction problems with multiple contacts. *The ANZIAM Journal*, 37(3):288–308, 1996.
- [37] David E Stewart and Mihai Anitescu. Optimal control of systems with discontinuous differential equations. *Numerische Mathematik*, 114(4):653–695, 2010.
- [38] Andreas Wächter and Lorenz T. Biegler. On the implementation of an interior-point filter line-search algorithm for large-scale nonlinear programming. *Mathematical Programming*, 106(1):25–57, 2006.